# CHAPTER 7. DISLOCATIONS

## 7.1 The Onset of Permanent Deformation

Like many new scientific ideas, the linear defect called a *dislocation* came about in order to explain the discrepancy between the then-current theory of the stress threshold for permanent deformation in solids and experimental observation. In common with a few other scientific phenomena, dislocations were conceived many years before they were actually observed.

Permanent deformation of a solid, also called *plastic deformation*, involves the slippage of one block of atoms over another block by a distance of roughly one atomic spacing. Figure 7.1 illustrates the fundamental distinction between elastic and plastic deformation caused by an applied shear stress.

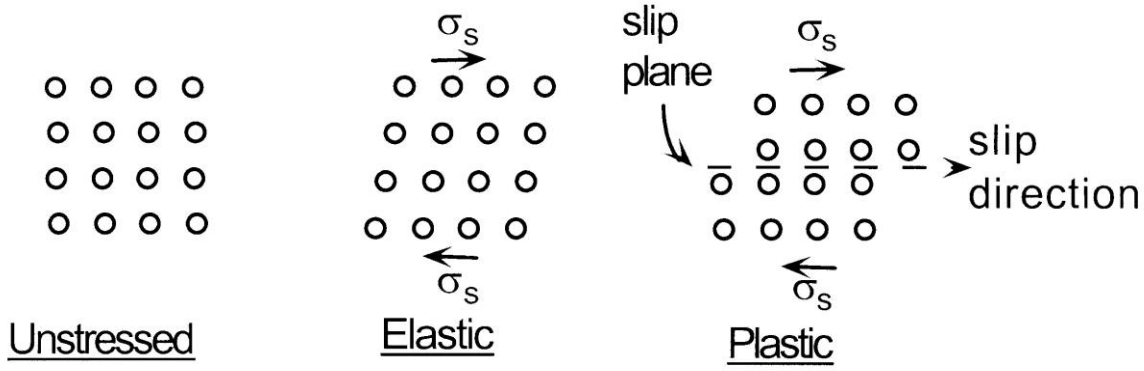


**Fig. 7.1 Schematic showing the distinction between elastic and plastic deformation due to an applied shear stress ($\sigma_S$).**

Elastic strain tilts or stretches the entire array of vertical atom planes without altering the relative positions of the atoms. *Plastic deformation* occurs at a higher shear stress and causes a portion of the solid to move, or *slip*, from the normal array to another normal configuration offset by approximately one lattice constant. Except for the steps at the sides, the atomic structure in the plastically-deformed solid is perfect. An important distinction between the two types of deformation is their reversibility: when the stress is removed, the elastically-deformed body returns to its original shape; a plastically-deformed body does not – the deformation is irreversible (see Chapter 11).

Suppose that the movement from left to right in Fig. 7.1 occurs by displacement of the entire block of atoms above the slip plane over the lower block in a single step. Such motion requires first an increasing system energy, reaching a maximum when the vertical atomic planes in the upper block are exactly midway between planes of the lower block. Continued motion from this position to the final position on the right in Fig. 7.1 is accompanied by reduction in system energy, which ultimately returns to the value in the unstressed solid. Since force is the negative of the derivative of the energy, and stress is force per unit area, this variation in energy implies a critical value of the shear stress at which the deformation switches from elastic to plastic. The

*theoretical shear strength* according to this mechanism is readily derived (see Ref. 1, p. 210; Ref. 2, p. 226, Ref. 3, p. 83, Ref. 4, p. 175, Ref. 5, p 11, Ref. 6, p. 1); it is predicted to be on the order of 0.1G, where G is the shear modulus of the solid (Eq (6.26)). This prediction is in fact obeyed only for very thin vapor-grown specimens called whiskers because these can be made dislocation free; for all other solids, including carefully-grown bulk single crystals, the "en bloc" model prediction is roughly four orders of magnitude larger than the *critical shear stress* observed in, say, a standard tensile test (Chapter 11). A discrepancy of this size naturally excites the imagination of theorists, three of whom independently invented the dislocation to rectify the disaccord (see Ref. 6, pp. 1 – 4 for this interesting bit of scientific history).

## 7.2 Dislocations

### 7.2.1 The Edge Dislocation

The theoretical notion of the microscopic entity called an *edge dislocation* has a macroscopic analog in the way a rug is moved. The left-hand sketch below suggests the considerable effort required to pull the entire rug over the floor; the next sketch shows that pushing a small wave-like section from one end to the other accomplishes the same displacement with a substantially reduced effort. The left-hand rug-pulling picture below is the analog of the "en bloc" model of the theoretical shear strength described in the preceding section; the right hand counterpart is the analog of the edge dislocation mechanism.

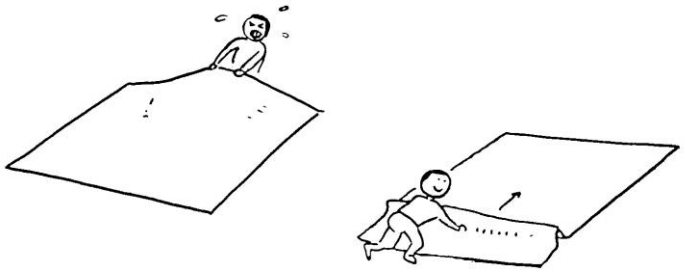

**The rug analogy**

In Fig. 7.2a, the applied shear stress causes the first column of atoms on the left and above the dashed horizontal plane to shift alignment from the first column below the plane to the second lower column, leaving a step on the left-hand face. This one-at-a-time switch in column alignment between the upper and lower atomic rows continues until the entire upper portion of the crystal has moved to the right by one lattice constant. The net deformation of the body is the structure in the bottom sketch of Fig. 7.2a, which is identical to that in Fig. 7.1. The horizontal plane separating the intact, stationary lower block of atoms from the displaced upper block is called the *slip plane*. The movement of the dislocation along this plane is termed *slip* or *glide*.

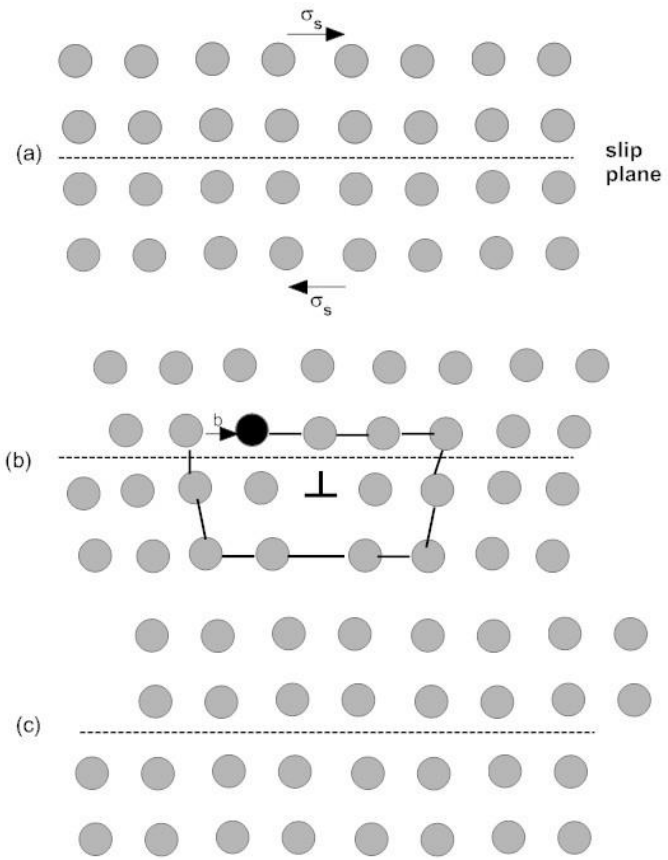


**Fig. 7.2a A schematic of the edge dislocation as it causes strain**

The diagram in the middle of Fig. 7.2a shows the structural configuration midway in the realignment process. An extra half-plane of atoms appears to have been inserted in the crystal, with its bottom edge terminating on the slip plane. Of course, the apparent extra half plane is just one of the existing upper planes pushed to the right. The termination of the extra half plane is the edge dislocation line on the slip plane, represented as an upside-down tee. If the extra half-plane had been inserted from the bottom of the diagram in the middle diagram of Fig. 7.2a, the tee would be drawn right side up. Such an edge dislocation would be of opposite sign as the one in Fig. 7.2a; one is termed *positive* and the other *negative.*

The shear stress needed to maintain motion of an isolated dislocation in a crystal with no nearby dislocations or other obstacle is called the *Peierls stress*. Its value is estimated at ~ $10^{-8}$G (Ref. 5, Sect. 10.2), which is many orders of magnitude lower than the measured stress need to sustain slip in annealed metals. In addition to most real materials being polycrystals requiring several slip systems to be operating simultaneously (see Chapter 11) the presence of obstacles such as other dislocations and of impurities ranging from atoms to large agglomerates is responsible for the actual stress required to cause slip in real single crystals to be higher than $10^{-8}$ G (Sect. 7.12).

### 7.2.2 The Screw Dislocation

The same deformation produced by the edge dislocation in Fig. 7.2a can be reproduced by a fundamentally different line defect termed the *screw dislocation*. This is depicted in Fig. 7.2b, but with the atoms represented by small cubes instead of spheres. The closest macroscopic analog of the shape change due to a screw dislocation is the tearing of a phone book.

The screw dislocation line is shown as the dashed line in Fig. 7.2b. Its name derives from the descending spiral experienced by tracing a circuit round the dislocation line following the original atom planes. When viewed end on, the screw dislocation is symbolized by **S**. Like the edge dislocation, screw dislocations can be right-handed or left-handed, depending on the direction of the spiral.

### 7.2.3 The Burgers Vector

A useful characterization of atomic distortions around a dislocation line is the *Burgers vector*. As the appellation "vector" suggests, it has both direction and magnitude. A simple

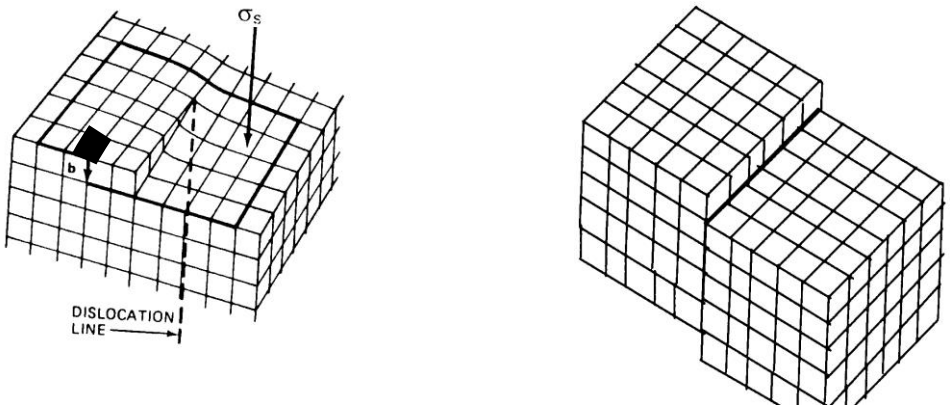


**Fig. 7.2b The screw dislocation in the simple cubic lattice**

method of determining the Burgers vector is indicated by the circuits around the dislocation lines indicated by the bold-line traces in Figs. 7.2a and 7.2b. In Fig. 7.2a, starting at the black atom and moving clockwise following the thick line by the same number of atoms left and right and up and down does not end on the starting atom. In each case the difference between the starting and end points after performing such a circuit is the Burgers vector. In Figs. 7.2a and 7.2b, the small arrows joining the starting and ending positions following these circuit are the Burgers vectors, denoted by $\vec{b}$. In the left-hand drawing of Fig. 7.2b, the circuit starting at the black cube terminates at a cube beneath the starting one.

Two other directional quantities characterize a dislocation: the direction of line movement $\vec{M}$ (the slip direction) and the direction of the line proper, $\vec{L}$ (the dislocation line).

The two basic dislocation types are shown in Fig. 7.3 and can be succinctly characterized by:

$$\underline{\text{edge}}: \quad \sigma_s \perp \vec{L}; \quad \vec{b} \perp \vec{L}; \quad \vec{M} \parallel \vec{b} \qquad \vec{M} \perp \vec{L};$$

$$\underline{\text{screw:}} \qquad \sigma_s \parallel \vec{L}; \quad \vec{b} \parallel \vec{L}; \quad \vec{M} \perp \vec{b} \qquad \vec{M} \perp \vec{L};$$

An important distinction is the second: the Burgers vector of an edge dislocation is *perpendicular* to the dislocation line while that of a screw dislocation is *parallel* to the line.

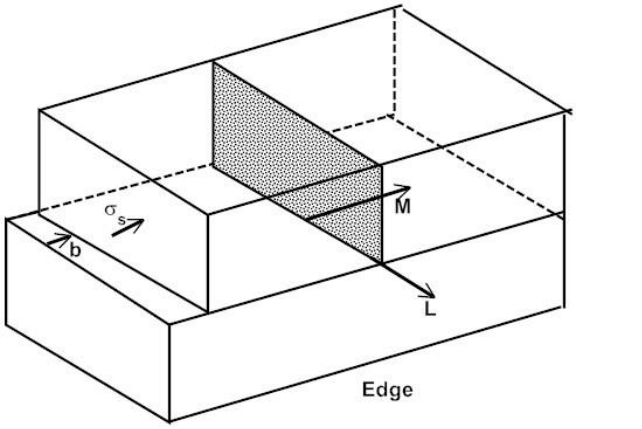


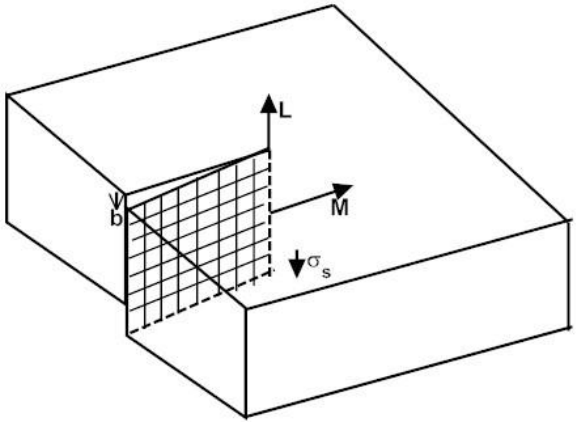


**Fig. 7.3 Direction of edge and screw dislocations**

The magnitude of the Burgers vector, b, for the simple cubic lattice, whether screw or edge, is equal to the lattice parameter $a_o$, the direction is [100], and the slip plane in which it moves is (100). The notation for this Burgers vector is:

$$\vec{b}_{sc} = a_o[100](100)$$

where the first term on the right is the magnitude of b, the second is the slip direction and the last term designates the slip plane. The generalization of this shorthand and of the magnitude of the Burgers vector for other lattice structures will be covered shortly.

## 7.3 Dislocations in Real Crystals

The preceding two sections used a simple cubic crystal structure to illustrate the basic features of dislocations. This particular lattice type is of no practical interest in elemental solids, since only elemental polonium exhibits this structure. In this work, the dislocation structure in the fcc elements is emphasized, with somewhat lesser attention paid to the bcc and hcp lattice types. Some information on dislocations in ionic solids can be obtained elsewhere (Ref. 5, p 120; Ref. 8, p. 152).

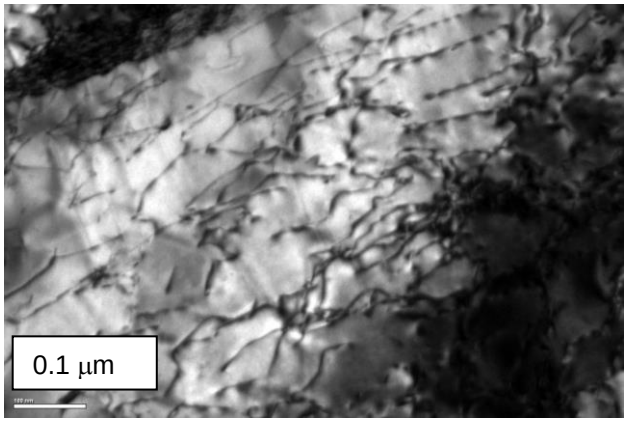


**Fig. 7.4 Transmission electron micrograph of the dislocation structure in NF616, a ferritic/martensitic alloy (C.Topbasi)**

The transmission electron microscope (TEM) image in Fig. 7.4 shows the complexity of the dislocation structure in a real metal. The dislocations (lines) are not straight, and appear to begin and/or end within the specimen, in this case because in the TEM what is examined is a very thin foil.

### 7.3.1 Slip systems

The lattice types of the more common metals are fcc, bcc, or hcp. In these structures, the slip planes, slip directions, and dislocation atomic configurations are more complex than in the simple cubic crystal. Pioneering tensile tests on oriented single crystals conducted in the 1930s revealed that for each lattice type, slip occurs on distinct *slip systems* defined by the *slip plane* and the *slip direction* which lies in the slip plane. As a general rule, slip occurs in a close packed plane, in the direction of the nearest neighbor. The closest packed plane in fcc is 111 and in that plane the nearest neighbor is in the 110 direction. As shown in Fig 7.6, in each 111 plane there

are three different 110 directions. Because there are four different 111 planes there are 4x3=12 different slip systems in fcc.

Figure 7.5 shows a single crystal, illustrated as an fcc crystal oriented and pulled along a [100] direction. Also shown is a (111) plane whose normal makes an angle $\phi$ with the imposed force direction, the [100] direction. The slip direction along the [110] makes an angle $\lambda$ with the same [100]. The angles in Fig.7.5 are treated in detail in Example #1 below.

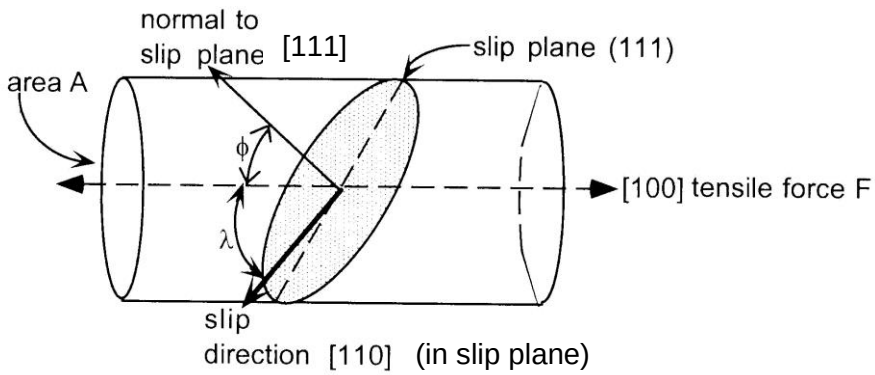


**Fig. 7.5 Slip characteristics in an oriented single crystal (fcc)**

In an fcc solid, movement by slip (i.e., by dislocation motion) always occurs on a (111) plane and in a [110] direction. In the fcc unit cell there are four (111) planes, each of which has three [110] directions. The distinct 4 x 3 = 12 combinations are individually termed the *slip systems*. The corresponding slip systems for fcc, bcc and hcp are shown in Fig. 7.6. In each case the slip direction is towards the nearest neighbor and in the closest packed plane.

Dislocations in each slip system are subject to a *resolved shear stress*. In the slip system shown in Fig. 7.5, the tensile force F creates a tensile stress $\sigma_{app} = (F/A)\cos\phi$ on the slip plane (shaded area $A/\cos\phi$). The shear component along the slip direction is this tensile stress times $\cos\lambda$. The *resolved shear stress* on the slip plane in the slip direction is:

$$\sigma_S = (F/A)\cos\phi\cos\lambda = \sigma_{app}\cos\phi\cos\lambda \qquad (7.1)$$

The shear stress at which slip first appears corresponds to a *critical resolved shear stress*, $\sigma_S^{crit}$. The factor $\cos\lambda\cos\phi$ is the *Schmid factor* for the particular slip system at that orientation. The slip system with the highest Schmid factor will be the first to operate. If the orientation of the specimen is changed (e.g., applied force changed from [100] to, say, [211]), slip initiation either occurs on another slip system with different $\phi$ and $\lambda$ or on the same slip system at a different applied stress $\sigma_{app}$[1]. However, $\sigma_S^{crit}$ calculated from Eq (7.1) is unchanged. This observation implies two features of slip in single crystals:

[1] Note that this is valid for a single crystal. For slip to occur in a polycrystal while maintaining strain compatibility requires the simultaneous operation of five independent slip systems causing the actual $\sigma_Y$ to be higher. This is at the origin of the Taylor factor discussed in Chapter 11.

| Crystal Structure | Slip Plane | Slip Direction | Number of systems | | Examples |
|---|---|---|---|---|---|
| bcc | {110} | <111> | 6x2=12 | 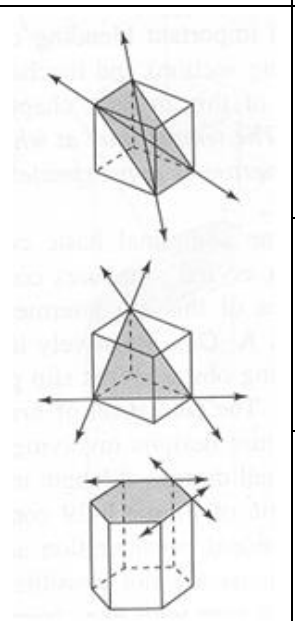 | a-Fe, Mo |
| fcc | {111} | <110> | 4x3=12 | | Al, Cu, Ni, g-Fe |
| hcp | (0001) | <1120> | 1x3=3 | | Zr, Ti |

**Fig. 7.6 Slip systems in the various structures (after Shackelford [10])**

1. The values of $\phi$ and $\lambda$ correspond to the member of the slip system that experiences the largest resolved shear stress
2. The orientation-independent value of $\sigma_S^{crit}$ represents the minimum shear stress to move an edge or screw dislocation in a particular lattice type. It is about $10^{-3}$ to $10^{-4}$ times smaller than the threshold shear stress computed from the "en bloc" model of permanent deformation described in Sect. 7.1.

Example #1 Slip-plane location (Fig. 7.7)

- Rather than $\phi$ and $\lambda$, computation of the resolved shear stress is simplified if a more manageable pair of angles is used. In addition to the polar angle $\phi$, the azimuthal angle $\varphi$ in the slip plane relative to the slip direction constitutes such a pair. Below we show how the resolved shear stress can be calculated for a given combination of $\phi$ and $\varphi$.
  The arrow OQ in Fig. 7.7 represents the applied stress $\sigma_{app}$ in Eq (7.1) and the procedure is as follows:
- $PQ = (OQ)\sin\phi$
- RPQ is an isosceles triangle; $\sin(\varphi/2) = \frac{1}{2}(RQ)/(PQ)$; $RQ = 2(OQ)\sin(\varphi/2)\sin\phi$
- $RS = OP = (OQ)\cos\phi$
- RSQ is a right triangle; $(SQ)^2 = (RS)^2 + (RQ)^2 = (OQ)^2[\cos^2\phi + 4\sin^2(\varphi/2)\sin^2\phi]$
- $OS = RP = PQ = (OQ)\sin\phi$

- Law of cosines for triangle OQS: $(SQ)^2 = (OS)^2 + (OQ)^2 - (OS)(OQ)\cos\lambda$
- Substituting SQ and OS and $\cos^2\phi = 1 - \sin^2\phi$; solving for $\cos\lambda$:

$$\cos\lambda = \sin(\phi)[1 - 2\sin^2(\varphi/2)] = \sin(\phi)\cos(\varphi)$$

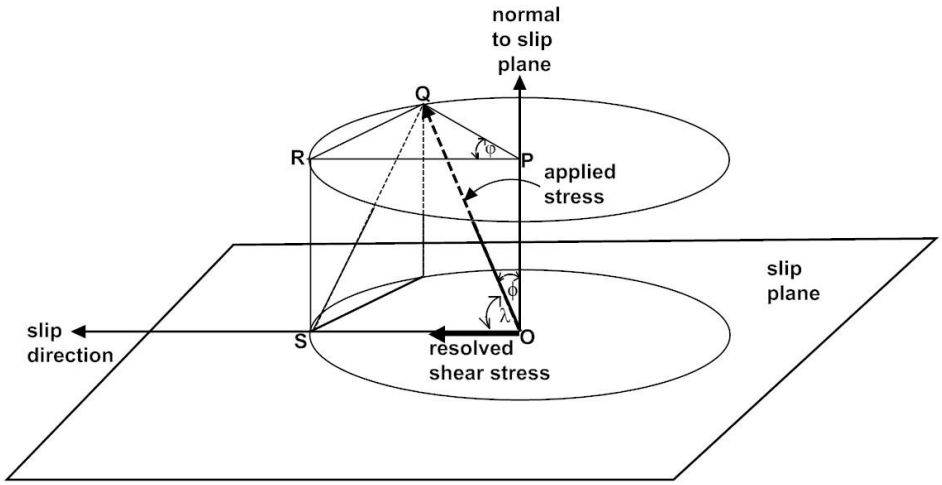


**Fig. 7.7 –resolved shear stress in a slip system**

Eliminating $\cos\lambda$ in Eq (7.1) gives the resolved shear stress in terms of the polar and azimuthal angles of the applied tensile stress relative to the normal to the slip plane ($\phi$) and to the slip direction ($\varphi$):

$$\sigma_S/\sigma_{app} = \sin(\phi)\cos(\phi)\cos(\varphi) \qquad (7.1a)$$

Plots of Eq (7.1a) for three values of the stress ratio are shown in Fig. 7.8. The curves represent combinations of $\phi$ and $\varphi$ that produce a specific $\sigma_S/\sigma_{app}$ ratio. The curves apply to any slip system.

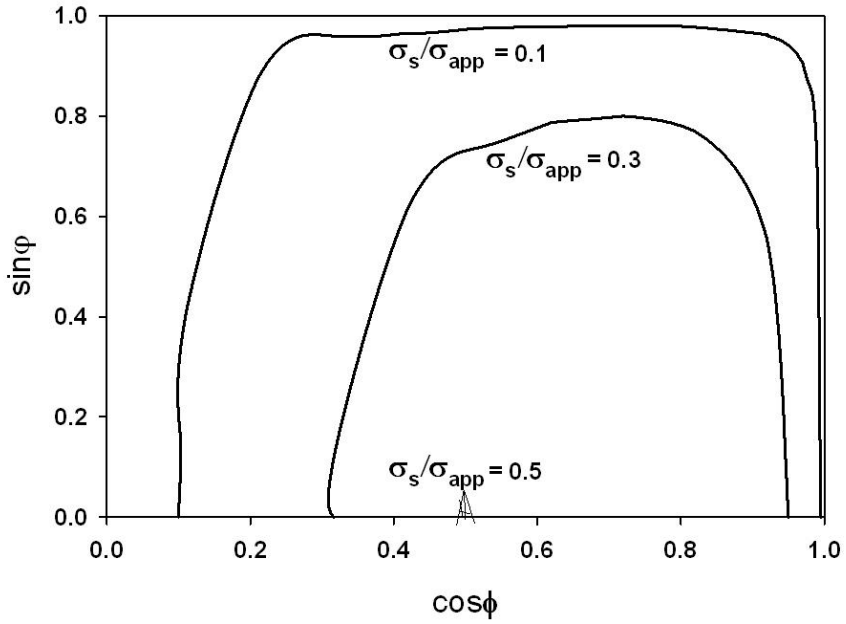


**Fig. 7.8 Plots of Eq (7.1a)**

The intersections of the curves on the abscissa identify the maximum and minimum values of cosϕ for which a given stress ratio can be obtained. $\sigma_S/\sigma_{app}$ ratios greater than 0.5 cannot be reached for any combination of ϕ and φ.

In other lattice types than fcc, the preferred slip directions and slip planes again follow the rule of nearest neighbor in the close packed plane, as shown in Fig. 7.6. In the bcc lattice, for example, slip occurs on (110) planes in [111] directions. Since there are six of the former and two of the latter, the bcc structure has 6 x 2 = 12 slip systems. Examination of the slip systems for the fcc and bcc lattice types suggests a generalization: slip occurs most easily on the closest-packed plane and in the closest-packed direction of the particular crystal structure. Both the fcc and bcc types follow this rule.

### 7.3.2 Compact Notation for the Burgers Vector

In order to completely characterize a Burgers vector, its direction and length need to be specified. The magnitude is determined by the b direction and the requirement that the minimum unit of slip reproduce the perfect lattice. As shown in the upper right-hand unit cell in Fig. 7.8, the magnitude of the Burgers vector for fcc slip is one-half of a face diagonal, or $b = a_o/\sqrt{2}$. The Burgers vector is denoted by: $\vec{b} = c[ijk]$, where i, j, and k are the Miller indices of its direction. The constant c is determined by the magnitude of $\vec{b}$ according to: $c = b/\sqrt{i^2 + j^2 + k^2}$ Thus for the fcc Burgers vector, substitution of $a_o/\sqrt{2}$ for b and i = 1, j = 1, k = 0 yields $c = (a_o/\sqrt{2})/\sqrt{2} = a_o/2$. The Burgers vector for fcc is designated as $a_o/2$ [110]. Even though the three arrows in the fcc structure in Fig. 7.6 have different directions, they are all the same kind of Burgers vector denoted by $a_o/2$ [110]. For completeness, the plane in which the dislocation (and hence the Burgers vector) lies is appended to the preceding notation. For the fcc structure, the Burgers vector of both screw and edge dislocations is:

$$\vec{b}_{fcc} = \frac{a_o}{2}[110](111) \qquad (7.2a)$$

In the bcc structure, the close-packed plane in which the Burgers vector lies is (110), and the close-packed direction in which it points is [111]. The length of the Burgers vector in this lattice is the distance between the central atom in the unit cell and a corner atom, or $b_{bcc} = (\sqrt{3}/2)a_o$ and the value of $c = (\sqrt{3}/2)a_o/\sqrt{1^2 + 1^2 + 1^2} = a_o/2$. The Burgers vector is:

$$\vec{b}_{bcc} = \frac{a_o}{2}[111](110) \qquad (7.2b)$$

This means a dislocation with a Burgers vector in the 110 direction, with a modulus of $a_o/\sqrt{2}$ and slipping in the 111 plane. Two dislocations of comparable energy are found in the hexagonal lattice structure. Dislocations in the basal plane (the (0001) plane, see Sect. 3.7.1) are most common. As in the fcc structure, which the hcp type closely resembles, the Burgers vector points

in the directions along the six sides of the hexagon, one of which is the $[11\bar{2}0]$ direction. Note (Fig.7.6) that the multiplicity of slip systems is much smaller in hcp (only three independent slip systems available) which makes slip quite a bit more difficult and enables other deformation mechanisms such as twinning to play a role (See Chapter 11). The designation of this dislocation is:

$$\vec{b}_{hcp}^{basal} = \frac{a}{3}[11\bar{2}0](0001) \qquad (7.2c)$$

Dislocations of the same direction lie in prism $(10\bar{1}0)$ planes as well. These dislocations are designated as:

$$\vec{b}_{hcp}^{prism} = \frac{a}{3}[11\bar{2}0](10\bar{1}0) \qquad (7.2d)$$

The method of determining the Burgers vector of the 4 – digit Miller planes is different than for the 3-digit technique described above for the cubic crystals. The 4-digit method is described in p. 107 of Ref. 6 and p. 108 of Ref. 7.

### 7.3.3 Mechanism of dislocation movement

The dislocations denoted by Eqs (7.2a) – (7.2d) are called *perfect* dislocations because the atom movement they represent reproduces the crystal structure without leaving a trace of its passing. However, the mechanism of this motion is not as straightforward as the simple shift of a half plane of atoms, as indicated in Fig. 7.2 for the sc lattice. As shown in Fig. 3.10, the fcc structure consists of stacking of (111) planes in an ABCABC… sequence. The mechanism of atom

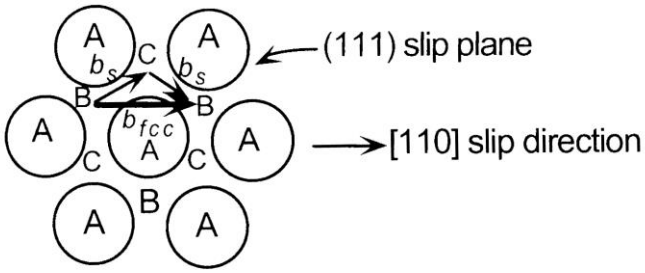


**Fig. 7.9 The slip mechanism in fcc crystals**

shifting during slip in the fcc structure in Fig. 7.9 shows an A layer in the familiar hexagonal pattern of the close-packed plane. The B and C layers above the A layer are not shown as circles; instead, the positions of the centers of these layers in the interstices of the A layer are indicated by letters. Slip consists of movement of the B layer (and all layers above) relative to the A layer (and all layers below) in a manner that reproduces the original perfect stacking sequence. The overall displacement is shown in Fig. 7.9 as the heavy arrow connecting the two B sites. However, the actual movement is the two-step path from B site to a C interstice and then to the next B site. This path is favored because the energy barrier of a direct B-to-B movement over the A layer is higher than the path following the two saddles between B and C and C and B. This can be appreciated by trying the two movements with ball models of close-packed (111) planes.

In other terms, the perfect dislocation $b_{fcc}$ splits into two *partial* dislocations labeled $b_s$ in Fig. 7.9. This process is called *dissociation*, and is written as a reaction:

$$\frac{a_o}{2}[110](111) = \frac{a_o}{6}[211](111) + \frac{a_o}{6}[12\bar{1}](111) \qquad (7.3)$$

$$B \rightarrow B \qquad B \rightarrow C \qquad C \rightarrow B$$

The two partial dislocations on the right hand side of this reaction are called *Shockley partial dislocations*. They represent the displacements from B to C and C to the next B. The sum of the energy of the partial dislocations can be smaller than that of the single perfect dislocation.

The perfect dislocations for the bcc and hcp structures given by Eqs (7.2b) – (7.2d) also undergo similar multiple-step atom displacements.

A useful view of edge dislocations is along the direction perpendicular to the slip plane. What has been loosely referred to as an extra "half plane" of atoms is an accurate description of the actual structure only for the sc lattice. This is so because this lattice consists of layered (100) planes. The top diagram in Fig. 7.10 shows the simple cubic lattice viewed in this manner. The atoms marked with an **X** represent the termination of the half plane, which is the row of atoms just above the inverted tee in Fig. 7.2.

The stacking sequences are different for the other cubic structures. Additionally, the repetitive nature of the stacking of planes for a particular lattice type depends upon which planes are involved. In the fcc lattice, for example, the common view is of a series of (111) planes placed above each other in an ABCABC… sequence (Fig. 3.5). However, the fcc lattice can also be reproduced by stacking (110) planes in an ABAB… pattern. Since the (110) planes are perpendicular to (111) planes, they constitute the extra half planes whose termination is the edge dislocation with the Burgers vector of Eq (7.2a). The middle sketch in Fig. 7.10 shows the two (110) half planes that constitute the edge dislocation. The terminating atoms are connected by a heavy line, indicating that the "half plane" is corrugated rather than flat.

The bcc structure can be constructed by stacking (111) planes in an ABCABC… sequence. Thus three (111) half planes constitute the edge dislocation in this lattice. The corrugation of the "half-plane" is even more pronounced than in the fcc structure.

### 7.3.4 Climb and Cross Slip

So far the only dislocation motion permitted was along its slip plane. Solids contain a variety of obstacles that effectively halt dislocation glide (i.e. slip). Among these are precipitate particles, bubbles or voids, grain boundaries, or other dislocations that are immobile because part of them lie out of their slip planes. If a mobile dislocation is pushed by a shear stress into one of these obstructions, one of three events occur:

1. The mobile dislocation is stopped
2. The mobile dislocation "cuts through" or "bends around" the obstacle
3. The mobile dislocation moves to another slip plane that is parallel to the original slip plane, on which it can continue to glide

The ability of a dislocation to evade the obstacles in its path is crucial to plastic deformation; if dislocations did not possess this flexibility, they would become immobile and plastic flow would cease.

Movement of an edge dislocation from one slip plane to a parallel one takes place by a mechanism called *climb* (No. 3 above). The extra half plane of atoms that constitutes the dislocation grows or shrinks by absorbing vacancies or interstitials from the bulk solid. The vacancy case is shown in Fig. 7.11.

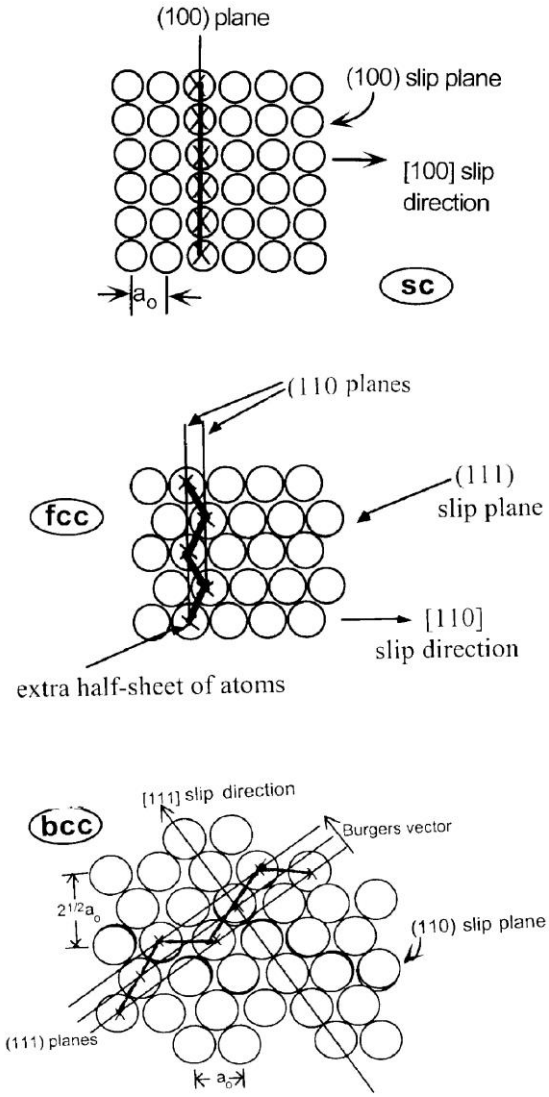


**Fig. 7.10 Extra half planes constituting the edge dislocation in cubic structures**

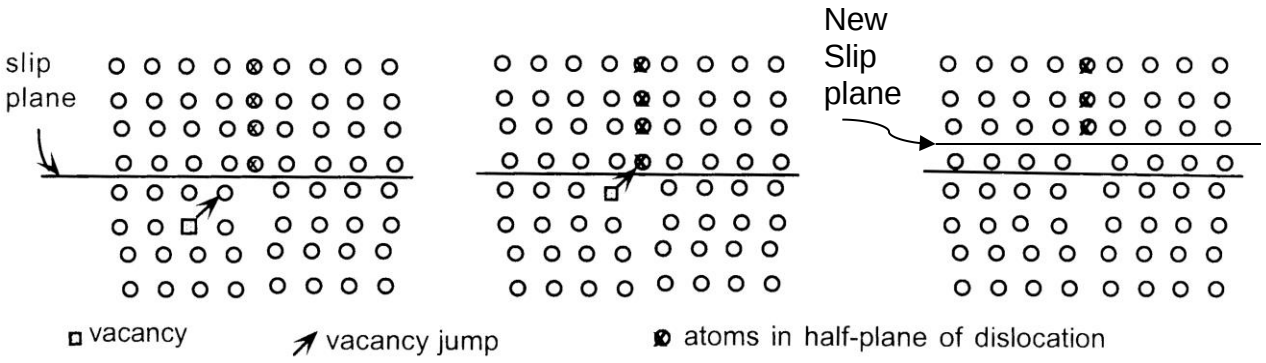


**Fig. 7.11 Mechanism of edge dislocation climb by vacancy absorption**

The first panel shows a vacancy making a random jump into a lattice site adjacent to the bottom of the half plane of atoms constituting the dislocation. Once in this location, exchange of the vacancy with the bottom atom of the dislocation (middle panel) is certain because of favorable energetics. If this happens all along the dislocation line (perpendicular to the page), the dislocation will have "climbed". The third panel shows the end result – the dislocation has "climbed" to a new slip plane parallel to the original one.

Climb of an edge dislocation perpendicular to its slip plane is a form of motion fundamentally different from the glide motion shown in Fig. 7.2. Because climb requires mobility of vacancies in the lattice, it is active only at high temperatures (say, ≥1/3 of the melting point) while slip has little temperature dependence and is the sole mechanism of edge dislocation movement at room temperature.

Climb of edge dislocations can also be mediated by interstitials. In this case, absorption of interstitials at the bottom of the half plane of atoms causes the dislocation to move downward instead of upward. This process is of no significance in unirradiated metals because of the very low concentration of interstitials at thermodynamic equilibrium (Chap. 3). However, irradiation by high-energy neutrons in a nuclear reactor displaces atoms from their normal lattice positions, creating equal numbers of interstitials and vacancies which can be absorbed at dislocations (Chap. 12 and 13).

Screw dislocations also absorb or emit point defects. However, rather than moving away from the slip plane, they develop a helical shape while remaining stationary.

Edge dislocations are constrained to move on the slip plane perpendicular to the termination of the extra half plane of atoms. Although there are a number of distinct slip planes of different orientation – four (111) in the fcc lattice, Fig. 7.8, and six (110) in the bcc structure – an edge dislocation on one type of slip plane cannot change to another. This restriction does not apply to screw dislocations. Because the slip planes in cubic lattices intersect, the screw dislocation can move from one to another, provided that the line of intersection of the slip planes is parallel to the screw dislocation.

Example #2: Cross slip of a screw dislocation A screw dislocation with its line in the $[1\bar{1}0]$ direction moves on the (111) plane.

Of the remaining nonparallel close-packed planes, only the $(11\bar{1})$ (lower right cube) intersects the (111) at a line in the $[1\bar{1}0]$ direction. This is best seen by examining the $(1\bar{1}0)$ plane labeled ABCD in the cube in the lower right of Fig. 7.8 in more detail on Fig. 7.12. .

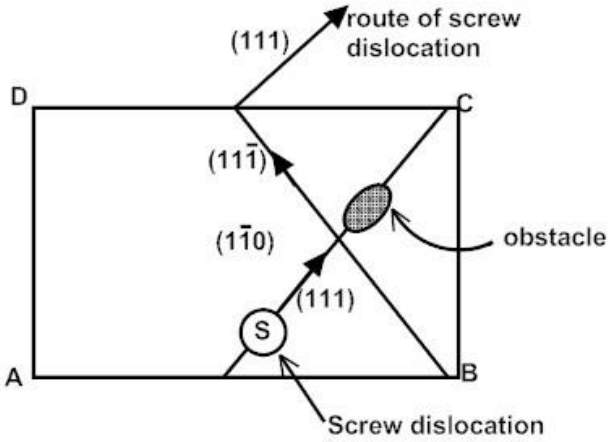


**Fig. 7.12 Cross slip of a screw dislocation in the fcc lattice**

As shown by application of Eq (3.6), the {111} planes are perpendicular to the $(1\bar{1}0)$ plane:

For $(1\bar{1}0)$ – (111): $$\cos^{-1}\left[\frac{(1)(1)+(1)(-1)+(0)(1)}{\sqrt{(1^2+1^2+0^2)(1^2+1^2+1^2)}}\right]=\cos^{-1}\left[\frac{0}{\sqrt{6}}\right]=90^o$$

For $(1\bar{1}0)$ – $(11\bar{1})$: $$\cos^{-1}\left[\frac{(1)(1)+(1)(-1)+(0)(-1)}{\sqrt{(1^2+1^2+0^2)(1^2+1^2+[-1]^2)}}\right]=\cos^{-1}\left[\frac{0}{\sqrt{6}}\right]=90^o$$

and the angle between the two (111) planes is:

(111) – $(11\bar{1})$: + $$\cos^{-1}\left[\frac{(1)(1)+(1)(1)+(1)(-1)}{\sqrt{(1^2+1^2+1^2)(1^2+1^2+[-1]^2)}}\right]=\cos^{-1}\left[\frac{1}{3}\right]=109.5^o$$

The screw dislocation line on the (111) plane in Fig. 7.12 (S) is perpendicular to the page and moves in the direction of the arrows. If, as shown, an obstacle is encountered on the (111) plane, the dislocation can switch to the $(11\bar{1})$ plane at their intersection. It moves with equal ease on both planes because the resolved shear stress responsible for its movement is parallel to the dislocation line (see Fig. 7.3), and is therefore the same on the (111) and $(11\bar{1})$ slip planes. The dislocation can switch back to a (111) plane, as shown in Fig. 7.12. This process is called *cross-slip.*

## 7.4 Dislocation Density

Defining a measure of the "concentration" of dislocations in a solid is not as straightforward as it is for discrete objects such as precipitates or bubbles. For the latter, the number of objects per unit volume, or number density, is a perfectly satisfactory gauge of their concentration.

Since most dislocations (not necessarily straight) start at one surface of a body and terminate at another surface, counting their number per unit volume not an option. Instead, the measure of dislocation concentration is defined as the total length of dislocation lines (including loops) per unit volume. This unit is called the *dislocation density*. This quantity is denoted by ρ and has units of $cm/cm^3$, or $cm^{-2}$. This quantity can be determined by measuring the length of the dislocations in TEM images, such as the one in Fig. 7.4.

There are a number of theoretical models of processes involving dislocations, including diffusion of point defects, creep mechanisms, and plastic yielding. For modeling purposes, the chaotic distribution of the dislocations seen in Fig. 7.4 must be greatly simplified.

The most common method of converting the randomness of the actual dislocation structure is shown in Fig. 7.13. On the left, the dislocations are treated as straight lines

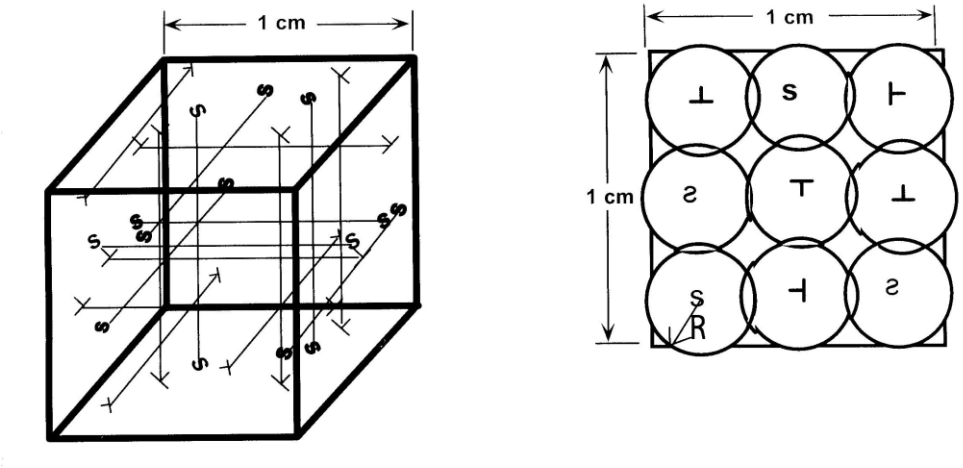


**Fig 7.13 Simplified model of dislocation lines in a solid**

extending from one face of a unit cube to the opposite face. All dislocations between a particular pair of opposing faces are assumed parallel. There are equal numbers of lines joining the other two faces of the unit cube. Both edge and screw dislocations are included, but there is no attempt to distinguish between them in reporting the dislocation density. Each dislocation segment in the unit cube is 1 cm in length, so the total number of segments is equal to the dislocation density.

The right-hand sketch in Fig. 7.13 shows the dislocations emerging at one face of the cube. Instead of random intersections, the terminations of the dislocations are arranged on a uniform square lattice. The circles around each dislocation represent the unit cell; that is, a structure that

is replicated throughout the solid. The circles are the ends of the cylinders of radius **R** with the dislocation on the axis. The number of unit cells per $cm^2$ is $\rho/3$, the remaining 2/3 of the dislocation belonging to the two other orthogonal directions. Note that $\rho$ has units of $cm^{-2}$, and can be thought of as the total length of dislocation line (cm) per volume ($cm^3$).

The unit cell radius is chosen so that the sum of the areas of the circles just fills the unit square. Since there are $\rho/3$ dislocations/$cm^2$, the reciprocal is the area associated with each dislocation, or the area of the unit cell is: $\frac{1}{\rho/3} = \pi \mathbf{R}^2$. Solving for the unit cell radius yields:

$$\mathbf{R} = \sqrt{\frac{3}{\pi\rho}} \tag{7.4}$$

Interaction between the cylindrical unit cells from one pair of unit cube faces with the unit cells from the other orthogonal faces is neglected, although in reality these must intersect each other. For example, in a metal with $\rho = 10^{10}$ $cm^{-2}$, Eq (7.4) gives $\mathbf{R} = 10^{-5}$ cm, or the dislocations are separated by roughly 0.2 μm. Without the very severe simplifications contained in Eq (7.4), it would be impossible to analyze many important processes involving point defects and dislocation lines.

Complete elimination of dislocations from a metal is neither possible nor desirable; dislocations are responsible for the strength of structural metals. They are produced in a metal by plastic deformation during fabrication and subsequent processing or in service. The dislocation density can be changed (within limits) by post-fabrication treatments such as cold-working, which increases $\rho$ by plastic deformation, or annealing, which decreases $\rho$ by permitting the thermodynamic tendency to eliminate defects to take place. The wide variety of processing methods available allows for control of the dislocation density over up to a 12-order of magnitude range. Table 7.1 shows typical values of $\rho$ for various materials.

**Table 7.1 Dislocation Densities of Various Materials**

| Material | Dislocation density, $cm^{-2}$ |
|---|---|
| Vapor-grown thin whiskers | <1 |
| High-purity silicon single crystals | $10^3$ |
| Annealed metals | $10^8$ |
| As-fabricated metals | $10^{10}$ |
| Cold-worked metals | $10^{12}$ |

## 7.5 Stress Fields Around Dislocations

The crystal lattice in the vicinity of a dislocation is distorted (strained). The strains produce stresses that can be calculated by elasticity theory beginning from a radial distance about 5b, or ~ 1.5 nm from the axis of the dislocation (Ref. 6, p. 36). Within this zone, called the *dislocation core*, the strains are too large for elasticity theory to be valid; interatomic-force calculations are required. Fortunately, the core contributes only minimally to phenomena involving the atomic

distortions due to the presence of the dislocation and is universally ignored in calculating the consequences of the stresses around dislocations.

The stress field around a dislocation is responsible for several important interactions with the environment. These include:

1. An applied shear stress on the slip plane exerts a force on the dislocation line, which responds by moving or changing shape.
2. Interaction of the stress fields of dislocations in close proximity to one another results in forces on both which can be either repulsive or attractive.
3. Edge dislocations attract and collect interstitial impurity atoms dispersed in the lattice. This phenomenon is especially important for irradiation-produced self-interstitials in metals exposed to high-energy neutron fields.

The geometry of the directions and planes in which the stress acts are covered in detail in the Appendix of this chapter.

### 7.5.1 Screw Dislocation

The screw dislocation has a much simpler stress field in the solid around it than does the edge dislocation. Figure 7.14 shows the distortion of a solid with a screw dislocation in the z direction. The circuit of radius r in the θ direction shown in the diagram is beyond the radius of the dislocation core, so the displacement in the z direction is the Burgers vector b. For $\theta < 2\pi$, the z displacement is:

$$u_z = b\frac{\theta}{2\pi} \tag{7.5a}$$

The shear strain $\varepsilon_{\theta z}$ is in the z direction and in the plane perpendicular to the θ arrow. This strain is related to $u_z$ by part of the group of relations given in brief by Eq (6.8):

$$\varepsilon_{\theta z} = \tfrac{1}{2}\left(\frac{du_\theta}{dz} + \frac{1}{r}\frac{du_z}{d\theta}\right) \tag{6.8a}$$

As can be seen from Fig. 7.14, there is no displacement in the θ direction ($u_\theta = 0$) and $du_z/d\theta$ is obtained from Eq (7.5a). The result is $\varepsilon_{\theta z} = b/4\pi r$

The corresponding shear stress is (see Eq (6.23)):

$$\sigma_{\theta z} = \frac{Gb}{4\pi r} \tag{7.5b}$$

All other stress components are zero. The stress field of Eq (7.5b) is axisymmetric about the dislocation line and falls off as $r^{-1}$. In Cartesian coordinates, two shear stress components are nonzero:

$$\sigma_{xz} = -\frac{Gb}{4\pi}\frac{\sin\theta}{r} \qquad \sigma_{yz} = \frac{Gb}{4\pi}\frac{\cos\theta}{r} \tag{7.5c}$$

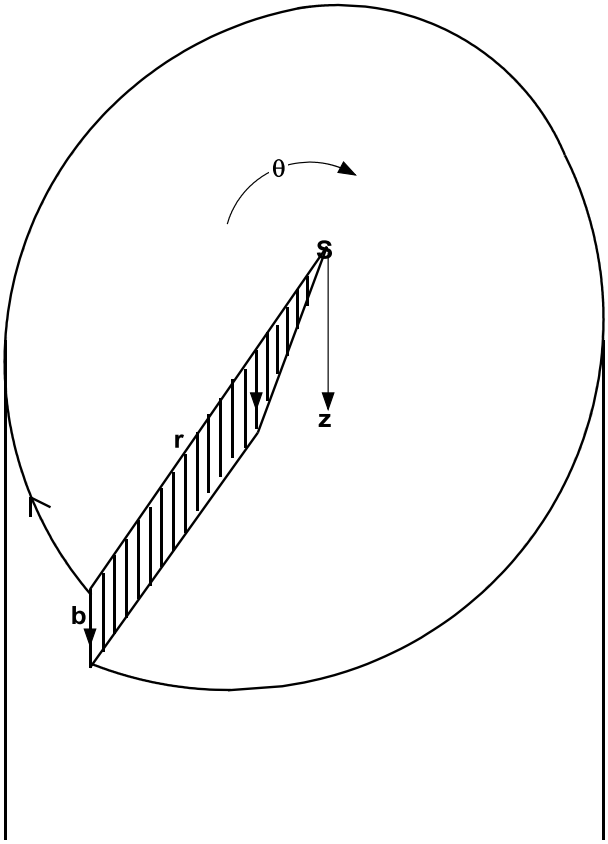


**Fig. 7.14 Displacement around a screw dislocation**

### 7.5.2 Edge Dislocation

In cylindrical coordinates the stresses around an edge dislocation are (Ref. 7, p. 37):

$$\sigma_{rr} = \sigma_{\theta\theta} = -\Gamma \frac{\sin\theta}{r} \qquad \sigma_{zz} = -2\Gamma\nu \frac{\sin\theta}{r} \tag{7.6}$$

$$\sigma_{\theta\, r} = \Gamma \frac{\cos\theta}{r} \tag{7.7}$$

The two remaining shear stress components are zero. The coefficient $\Gamma$ is:

$$\Gamma = \frac{Gb}{2\pi(1-\nu)} \tag{7.8}$$

In rectangular coordinates, Eqs (7.6) and (7.7) are:

$$\sigma_{xx} = -\Gamma \frac{\sin\theta\,(1+2\cos^2\theta)}{r} \qquad \sigma_{yy} = -\Gamma \frac{\sin\theta\,(\cos^2\theta - \sin^2\theta)}{r} \tag{7.6a}$$

$\sigma_{zz}$ is unchanged.

$$\sigma_{yx} = \Gamma \frac{\cos\theta\,(\cos^2\theta - \sin^2\theta)}{r} \qquad (7.7a)$$

## 7.6 Dislocation self-energy

The stress field around a dislocation produces elastic strain energy (Eq (6.31)). This energy, which is referenced to that of the perfect crystal, is the reason that the dislocation is a non-equilibrium object..

The elastic strain energy of dislocations is of interest for two reasons: first, it determines the type of dislocation in a particular crystal type; and second, it determines the response of a pinned, or immobile, dislocation to applied stresses.

The elastic strain energy around a screw dislocation is easy to derive because only one stress component is generated in its vicinity. Letting 2 = θ and 3 = z in Eq (6.31), all terms except the last are zero. Substituting Eq (7.5b) into this term gives:

$$E_{el} = \frac{Gb^2}{32\pi^2 r^2} = \frac{energy}{unit\ volume} \text{ at distance r}$$

A volume element $2\pi r dr$ is chosen and the above equation is integrated to give the total energy per unit length of dislocation:

$$E_{dis} = E_{core} + \int_{r_o}^{R} 2\pi r E_{el} dr = E_{core} + Gb^2 \left[ \frac{\ln(R/r_o)}{16\pi} \right] \qquad \text{[J/m]}$$

where $E_{core}$ is the energy of the core of the dislocation ($0 \le r \le r_o$). The limits on the integral are the radial extremes of the unit cell shown in the right-hand diagram in Fig. 7.13. The lower limit is the core radius of the dislocation, and the upper limit is the radius of the unit cell given by Eq (7.4). Assuming the bracketed term to be about unity and neglecting the contribution of $E_{core}$ gives the dislocation's self energy per unit length as:

$$E_{dis} = Gb^2 \qquad (7.9)$$

$E_{dis}$ for an edge dislocation is obtained by substituting Eqs (7.6) and (7.7) into Eq (6.31), i.e. $E_{dis} = Gb^2/(1-\nu)$ for edge dislocations. The result differs from $E_d$ for a screw dislocation by the term (1 - ν) in the denominator, where ν is Poisson's ratio. Since 1 - ν ~ 2/3, the coefficient of $Gb^2$ is increased by ~ 50% over that of a screw dislocation. This change is within the uncertainty of the coefficient of $Gb^2$, so Eq (7.9) is applied to both edge and screw dislocations.

Just as the energy per unit area of a surface acts as a surface tension, so the energy per unit length of a dislocation ($E_d$) can be treated as a *line tension*. This aspect of the dislocation self-

energy comes into play when a curved section of a dislocation is acted upon by an applied stress. The loop shown in Fig 7.5, for example, is maintained by a dynamic balance between the shrinkage tendency of the line tension and the expansion tendency of the applied shear stress. If the latter were removed, the line tension would cause the loop to shrink until the dislocation segments of opposite sign at the extremities of a diameter met and annihilated each other. The loop would simply vanish.

The other important feature of Eq (7.9) is the dependence of $E_d$ on b. The smaller the Burgers vector, the lower the dislocation self-energy. Consequently, the energetically most favorable dislocation is the one that points in the direction of the closest-packed atomic row of the crystal structure as discussed above. The size of this dislocation is the distance between adjacent atoms.. This "rule" can be seen in the Burgers vectors drawn on the fcc lattice in the upper right hand cube in Fig. 7.8. The Burgers vector for the bcc structure (Eq 7.2b) and for the hcp lattice (Eqs (7.2c) and (7.2d)) also obey the smallest-b "rule".

## 7.7 Stresses to Initiate Dislocation Movement

In order to start a dislocation moving on its slip plane, a sufficiently large shear stress must be applied. The magnitude of this stress depends upon the microstructure of the solid. The resistance to initiation of dislocation movement is due to:

i) impurity atoms near to or attached to the dislocation;
ii) the presence of nearby or intersecting dislocations;
iii) pinning of dislocations at points where they leave their slip planes.

Despite the inherent variability of these impediments to dislocation motion, high-purity single crystals exhibit a critical resolved shear stress $\sigma_S^{crit}$ (Sect. 7.3.1)) that is sufficiently reproducible to be considered a property of the metal[2].

The origin of the intrinsic resistance to slip of a straight dislocation line in a perfect crystal can be inferred from the motion of the plane of atoms illustrated in Fig. 7.2 for an edge dislocation. The upper half-plane of atoms appears to move to the right because the atomic row below the slip plane and to the right of the dislocation switches alignment to the upper half-plane. In so doing, a small energy barrier must be surmounted. In effect, this periodic barrier to slip is a miniature version of the much larger periodic barrier required for slip by the *en bloc* mechanism (Sect. 7.1). The stress required to move the dislocation by the mechanism of Fig. 7.2 in the hypothetical crystal of complete microstructural and compositional perfection is called the *Peierls stress*, $\sigma_P$. Although there are no experimental measurements of $\sigma_P$, there is no shortage of theoretical estimates of its magnitude. Unfortunately, there is no agreement as to the correct model[3].

[2] A list of $\sigma_S^{crit}$ for various materials is given on p. 228 of Ref. 4

[3] These theories are reviewed in Ref. 7, p. 147 et seq; see also Sect. 7.2

At the opposite extreme of the Peierls stress is the applied stress required for initiation of plastic deformation in commercial structural alloys. This is the *yield stress* $\sigma_Y$.

Table 7.2 summarizes the three characteristic stresses for initiation of dislocation motion in materials of varying purity.

**Table 7.2 Characteristic Stresses for Initiation of Dislocation glide (in order if increasing magnitude)**

| Name of stress | Symbol | Material Condition |
|---|---|---|
| Peierls | $\sigma_P$ | Perfect crystal; single straight dislocation |
| Critical resolved | $\sigma_S^{crit}$ | High-purity single crystal |
| Yield* | $\sigma_Y$ | Commercial product |

* see Sect. 7.12 for an explanation of yielding

Because of the dependence on the material and its microstructural condition, values of the characteristic stresses are not given in the table.

## 7.8 Forces exerted on dislocations by applied stresses

The types of stresses listed in Table 7.2 are produced by an applied shear stress on the slip plane containing the dislocation. As shown in Fig. 7.2, the dislocation moves to the right if the applied shear stress $\sigma_S$ above the slip plane points in the direction of the Burgers vector. This situation is shown in detail suitable for analysis in Fig. 7.15.

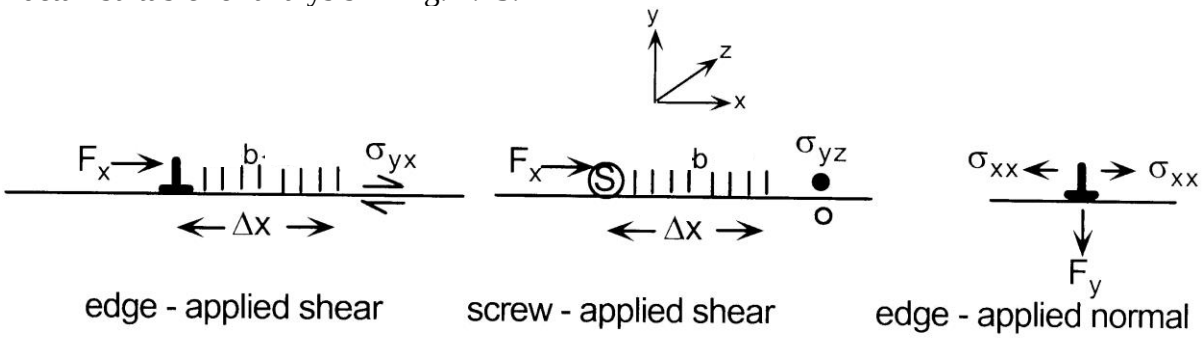


**Fig. 7.15 Diagrams for deriving forces on dislocations due to applied stresses. F is the force exerted on the dislocation in response to the applied stress**

### 7.8.1 Slip force on an edge dislocation

The edge dislocation on the left in the figure is acted upon by an applied shear stress in the slip plane and in the direction indicated. This shear stress is converted to a force per unit length by a force balance on the dislocation. To determine the $F_x$, the work to move the dislocation a distance $\Delta x$ is calculated in two ways.

1. The z-direction force applied to the area 1 x $\Delta x$ by the shear stress is $\sigma_{yx}\Delta x$. The distance over which this force acts is the Burgers vector b, because this is the length that the

atomic planes above the slip plane move as the dislocation passes. Thus, the work done by the shear stress in moving the dislocation a distance $\Delta x$ is:

$$W \text{ (due to shear stress)} = \sigma_{yx} \Delta x \, b$$

2. Alternatively, a hypothetical force $F_x$ acts on the unit length of dislocation line and moves it a distance $\Delta x$. The work done is:

$$W \text{ (due to force)} = F_x \, \Delta x$$

These two formulas for the work must be equal, which leads to::

$$F_x = \sigma_{yx} \, b \qquad (7.10)$$

### 7.8.2 Climb of an edge dislocation

Climb of an edge dislocation (Fig. 7.11) requires a normal stress acting in the direction shown in the right-hand sketch in Fig. 7.15. The work analysis in the previous section can also be applied to the normal stress. A positive normal stress (i.e. $\sigma_{xx}$ tensile) produces a force per unit length in the negative y direction:

$$F_y = - \sigma_{xx} b \qquad (7.11)$$

This force acts to drive the half-sheet of atoms downward in the diagram. This result can be viewed as follows: if the plane of atoms of the edge dislocation is regarded as a crack in a brittle solid, a tensile stress perpendicular to the crack causes it to propagate. The force given by Eq (7.11) results in climb of the dislocation only if a sufficiently large concentration of mobile point defects exists in the bulk of the solid. This requires either high temperature or a radiation field.

### 7.8.3 Slip of a screw dislocation

Figure 7.3 shows that the only shear stress that exerts a force on a screw dislocation is $\sigma_{yz}$. In the center diagram of Fig. 7.15, this shear stress is depicted as two circles above and below the slip plane, with the filled circle acting in the positive z direction. By an analysis identical to the one given above for the edge dislocation, the x force per unit length exerted on the screw dislocation is:

$$F_x = \sigma_{yz} \, b \qquad F_y = \sigma_{xz} b \qquad (7.12)$$

In this case, the stress component parallel to the dislocation line is the source of the force perpendicular to the line. This may appear counterintuitive, but examination of Fig. 7.3 suggests a simple analogy; when you tear a sheet of paper, you pull up and down perpendicular to the sheet and the paper rips in the direction perpendicular to the forces you exert on it (try it).

### 7.8.4 Climb of a screw dislocation

No diagram for the response of screw dislocation to a normal stress is shown in Fig. 7.15. The dislocation responds to normal stresses by coiling into a helical shape. However, there is no net motion of the dislocation, so this phenomenon is not of interest in explaining the mechanical properties of solids.

## 7.9 Interaction Forces Between Dislocations

The proximity of two dislocations results in forces between them. Depending on their relative positions and orientations, the interaction force may be positive or negative. A positive interaction force means that the two dislocations attract each other; negative interaction corresponds to repulsion. Knowledge of these interaction forces is useful in understanding mechanical properties of metals, including the onset of plasticity (yielding) and the rate at which one dislocation surmounts the repulsion of another (creep).

The stresses in Eqs (7.10) – (7.12) were said to be "applied", meaning generated by an external load on the body. However, they can originate from any source, in particular, the presence of a nearby dislocation. Figure 7.16 shows the simplest of the combinations of the relative positions of the two pairs of parallel dislocations, one pair screw of opposite sign and the other pair edge of the same sign.

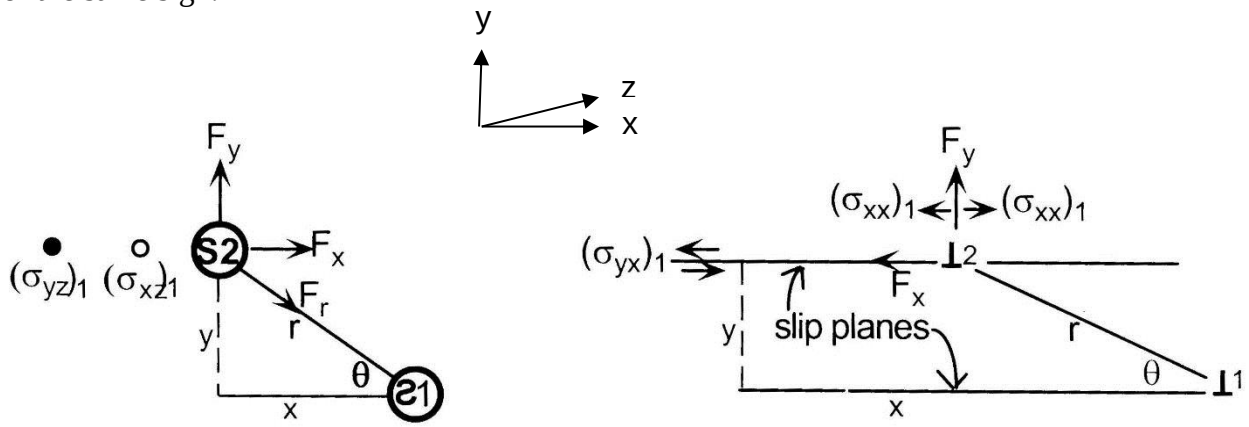


**Fig. 7.16 Interactions between two screw dislocations and between two edge dislocations**

### 7.9.1 Parallel Screw Dislocations

No slip planes are shown for the screw dislocations on the left in Fig. 7.16 because there are many slip directions available to this type of dislocation. However, interaction forces (per unit length of dislocation) in the x and y directions shown in Fig. 7.16 are readily calculated.

Substituting the second of Eqs (7.5c) into (7.12) yields:

$$F_x = \left(\sigma_{yz}\right)_1 b = \frac{Gb^2}{2\pi r}\cos\theta \qquad (7.13a)$$

Substituting the first of Eqs (7.5c) into the $F_y$ component of Eq (7.12) yields:

$$F_y = (\sigma_{xz})_1 b = -\frac{Gb^2}{2\pi r}\sin\theta \qquad (7.13b)$$

where the subscript 1 indicates that the stress component is generated by dislocation 1 at the location of dislocation 2. The interaction force in the line joining the two dislocations is obtained by resolving $F_x$ and $F_y$ in the r direction:

$$\text{component of } F_x \text{ along r} = F_x\cos\theta = \left(\frac{Gb^2}{2\pi r}\right)cos^2\theta$$

$$\text{component of } F_y \text{ along r} = -F_y\cos\left(\frac{\pi}{2} - \theta\right) = -F_y\sin\theta = \left(\frac{Gb^2}{2\pi r}\right)sin^2\theta$$

The sum of these two components is the radial interaction force:

$$F_r = \left(\frac{Gb^2}{2\pi r}\right) \qquad (7.14)$$

The interaction force between two parallel screw dislocations is along the line of connection perpendicular to both. $F_r$ is *attractive* if the two dislocations are of opposite sign and *repulsive* if they are of the same sign. The force on dislocation 2 due to the presence of dislocation 1 is equal and opposite to the force exerted by 1 due to 2, i.e. $F_{12}=-F_{21}$.

### 7.9.2 Parallel Edge Dislocations

The right-hand diagram in Fig. 7.16 shows two parallel slip planes separated by a distance y. The edge dislocations are constrained to move on these planes, in contrast to screw dislocations, which have a number of directions in which to move by slip.

The x-force on dislocation 2 due to the presence of 1 is obtained by substituting Eq (7.7a) into (7.10):

$$F_x = \Gamma b\frac{\cos\theta(\cos^2\theta - \sin^2\theta)}{r}$$

or, in compact form:

$$F_x = \Gamma b\frac{f_x(\theta)}{y} \qquad (7.15)$$

where $y = r\sin\theta$ is the separation of the slip planes, $\Gamma$ is given by Eq (7.8), and

$$f_x(\theta) = \sin\theta\cos\theta(\cos^2\theta - \sin^2) = \frac{1}{4}\sin(4\theta) \tag{7.16}$$

For the y-force exerted on dislocation 2 by dislocation 1, the first of Eqs (7.6a) is used in Eq (7.11), giving:

$$F_y = \Gamma b \frac{\sin^2\theta(1+2\cos^2\theta)}{y} = \Gamma b \frac{f_y(\theta)}{y} \tag{7.17}$$

The angular functions $f_x$ and $f_y$ are plotted in Fig. 7.17.

Both angular functions are zero when $\theta = 0$ which, for a fixed slip-plane separation y, means that the two dislocations are infinitely far apart. As dislocation 2 approaches dislocation 1, the $f_x$ function is positive. This means that $F_x$ is positive, or in the geometry of Fig. 7.16, the two dislocations repel each other. The maximum repulsion on the slip planes occurs at $\theta = \pi/8$, where $f_x = ¼$. Thereafter, the repulsive force decreases until the angular region between $\pi/4$ and $\pi/2$ (when the two dislocations are aligned along the y axis), where the interaction is attraction.

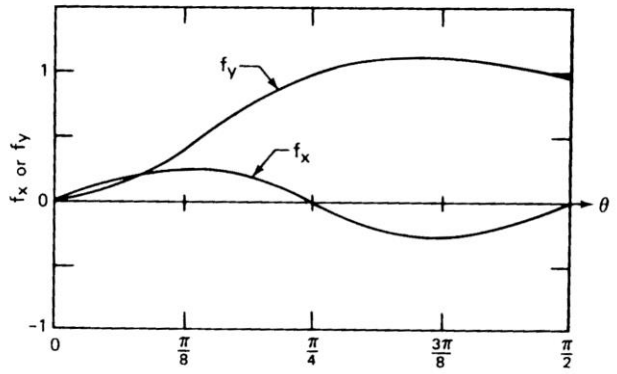


**Fig. 7.17 Angular dependencies of the forces between two parallel edge dislocations of the same sign**

The $f_y$ function is positive for all angles, meaning that dislocation 2 tends to be pushed upward, away from dislocation 1. This is intuitively correct; according to the first of Eqs (7.6a), the entire upper hemicylinder around the edge dislocation ($0 \le \theta \le \pi$) is in compression. The compressive normal stress tends to "squeeze out" the half plane of atoms constituting the edge dislocation, which is equivalent to an upward (y) force on the dislocation. The normal force $F_y$ is a driving force for climb of the dislocation, but whether this occurs depends on the mobility of the vacancies in the lattice, which in turn is highly temperature-sensitive.

The above analysis applied to parallel edge dislocations of the same sign. If the dislocation 1 in Fig. 7.16 were turned upside down (i.e., the half-plane coming in from the bottom instead of from the top), its Burgers vector would change sign. As a result, the curves in Fig 7.17 would also be flipped; the long-range $F_x$ force would be attractive but repulsion would set in for angles greater than $45^o$.

As in the case of the interaction of two screw dislocations, the x and y forces on dislocation 1 arising from the stress field of dislocation 2 are equal in magnitude but opposite in direction to the forces on 2 from 1.

### 7.9.3 Other combinations

The relative positions of the dislocations in Fig. 7.16 (both parallel) represent the simplest cases of dislocation interaction. Calculation of the interaction forces for other orientations is more complicated. The more complex situations include: parallel edge and screw; two parallel edge with perpendicular Burgers vectors; and perpendicular dislocation lines (Problems 7.10 – 7.12).

## 7.10 Equilibrium Dislocations

Dislocations are mobile because of the force acting upon them by the applied shear stress $\sigma_S$. Consider a mobile dislocation line: 1) in the z direction; 2) in a slip plane perpendicular to the y direction; 3) moving in the x direction. The x force on the mobile dislocation is given by Eq (7.10) for an edge dislocation or the first of Eq (7.12) for a screw dislocation. For the present purposes, these forces are rewritten as:

$$F_{app} = \sigma_S b \tag{7.18}$$

The mobile dislocation encounters an immovable obstacle and responds by either:

i) stopping and assuming a shape or position the creates a back force that just counterbalances the forward force $F_{app}$ (this section);

ii) breaking through or moving past the obstacle (next two sections).

Several examples of the force equilibrium that stops the mobile dislocation are given below.

### 7.10.1 Parallel Screw Dislocations

In Fig. 7.16a, dislocation S2 is driven to the right by an applied force $F_{app}$. The sign of S1 in Fig. 7.16 has been changed so that S1 and S2 now have the same sign. Then, instead of attraction, the two dislocations repel each other. S1 is assumed to be immobile and constitutes the obstacle to the motion of S2.

By changing the sign of S1, the direction of the $F_x$ in Fig. 7.16 is flipped by $180^o$. S2 is driven to the right in the figure with the forward force $F_{app}$ and the back force $F_x$ from S1 opposes it. S2 stops when the opposing forces just balance, or when $F_{app} = F_x$.

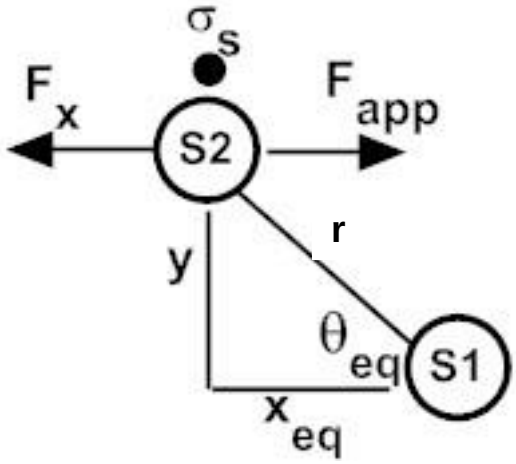


**Fig. 7.16a Equilibrium spacing of parallel screw dislocations**

Using Eqs (7.13a) and (7.18), this force balance becomes:

$$\sigma_S b = \frac{Gb^2}{2\pi r}\cos\theta \qquad (7.19a)$$

If the distance between the slip planes of S1 and S2 is a fixed, specified value y, the quantity of interest is $x_{eq}$ the separation of the two dislocations at equilibrium. Replacing r in the above equation by y/sinθ and using the trigonometric identity sin(2θ) = 2sinθcosθ results in:

$$\sigma_S = \frac{Gb}{4\pi y}\sin(2\theta_{eq}) \qquad (7.19b)$$

Example #3: If a shear stress equal to 1% of the shear modulus is applied to the mobile screw dislocation and the separation of the parallel slip planes of S1 and S2 is five Burgers vectors, what is $x_{eq}$? Using $\sigma_S/G = 0.01$ and $y/b = 5$ in Eq (7.19b) and solving gives $\sin(2\theta_{eq}) = 0.63$ or $\theta_{eq} = 19.5^o$. From the geometry of Fig. 7.16a, $x_{eq} = y/\tan\theta_{eq} = 14b$.

### 7.10.2 Bowed edge dislocation

An edge dislocation driven by an applied shear stress encounters a pair of point obstacles in its slip plane (shown as black dots in Fig. 7.18). If the portion of the dislocation line between the two pinning points is to attain an equilibrium shape, it must generate a back force to balance $F_{app} = \sigma_S b$. It does so by bowing out, as shown in Fig. 7.18. The extent of bowing, as measured by the radius of curvature ℜ, is obtained from a force balance in the upward direction. The applied force acts normal to the entire length of the curved segment, which is of mixed edge/screw character. The three dimensional analog is the gas pressure in balloon. The total upward force on the bowed dislocation is $F_{app}L = \sigma_S bL$, where L is the distance between pinning points.

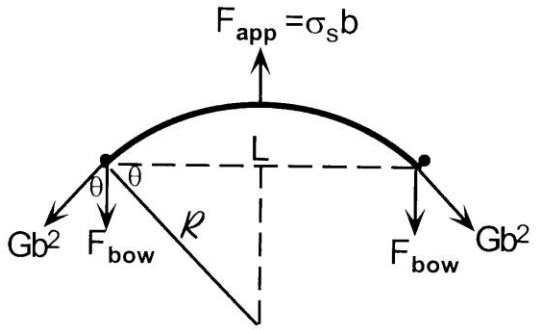


**Fig. 7.18 Force balance on a bowed dislocation**

The upward force is balanced by the line tension of the dislocation, which is the same as its elastic strain energy per unit length, $Gb^2$ (see Eq (7.9) et seq.). The line tension acts tangent to the bowed dislocation at the pinning points. The force resolved in the downward direction, shown as $2F_{bow}$ in Fig. 7.18, is $2Gb^2\cos\theta$. However, $\cos\theta = (L/2)/\Re$, so the downward force is $Gb^2L/\Re$. Equating the upward and downward forces leads to the radius of curvature at equilibrium:

$$\Re = Gb/\sigma_S \tag{7.20}$$

which is independent of the spacing of the obstacles that pin it. If the shear stress reduces the radius of curvature to L/2, the dislocation becomes a semicircle. Any larger shear stress separates the arc from the pinning points and converts it into a loop, as shown in Fig. 7.5.

### 7.10.3 Dislocation loop

Figures 7.2 and 7.3 suggest that dislocations are straight lines running through the entire length of the crystal. While the latter inference is correct, the former is not; dislocations can be of any shape, and need not lie in a single slip plane. However, they cannot start or stop inside the crystal.

If a dislocation line is curved, or a straight segment is neither pure edge nor pure screw, the dislocation line is said to be *mixed*, or part edge and part screw. Atomic representations of a curved dislocation are not particularly informative, but are given in Ref. 1, p. 105, Ref. 2, p. 83, and Ref. 7, p. 130. The important feature of the mixed dislocation is that it possesses a unique Burgers vector, irrespective of its shape.

Loops are closed curves whose periphery consists of a dislocation. The loop may or may not be planar, but here we consider only the plane version. They come in two types: a shear loop or a faulted loop.

*Shear loop*

In the first type, the crystal structure of the interior plane of the loop is perfect; the distortion caused by the shift of atoms is accommodated by the peripheral edge dislocation. The magnitude

of the shift is one atomic spacing in a simple cubic structure or the magnitude of the Burgers vector for other crystal types.

This type of loop is called a *shear loop* because it is produced by the action of a shear stress on the slip plane. Figure 7.19 shows a circular shear loop and the dislocations that constitute its periphery.

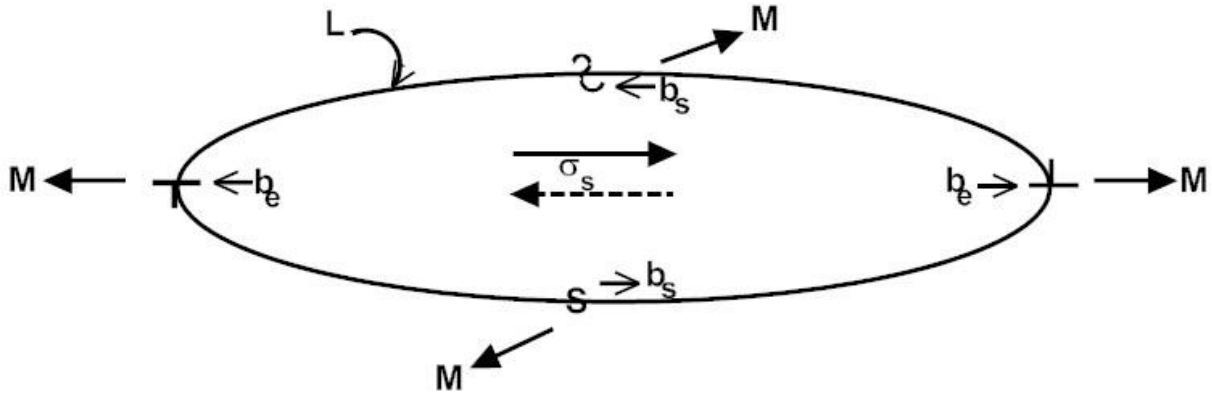


**Fig. 7.19 Dislocation components of a shear loop**

The pure edge and pure screw parts are present only at points on the circle $90^o$ apart. In between, the dislocation is mixed edge/screw, with the preponderant type changing from edge to screw and back as the circle is traversed. However, as shown by the M arrows, the direction of motion of the dislocation loop is outward throughout.

A remarkable feature of the shear loop, whether it be planar or nonplanar, circular or noncircular, is that, except for the sign, it is characterized by a single Burgers vector. In Fig. 7.5, the Burgers vector is perpendicular to the pure edge portions of the loop and parallel to the pure screw components. Only the directions of $\vec{b}$ are reversed between the negative and positive edge portions and the right-hand and left-hand screw parts. When a shear stress is applied to the slip plane in the sense of the pair of arrows in Fig. 7.19, the entire circumference of the loop expands (Sect. 7.8) until it leaves the crystal. The resulting permanent deformation is identical to the final block shift shown in Figs. 7.2 and 7.3.

*Prismatic or Faulted loop.*

In the second type, the loop is formed by removal or addition of a disk of atoms between close-packed atomic planes. For example, Fig. 3.10 shows the stacking sequence of close-packed planes in in the fcc lattice (abcabc…) and the hcp lattice (abab…). If one of these planes is removed, a *stacking fault* is created: (ab/abc in fcc, ab/bab in hcp). The periphery of these loops are also dislocations, although of a different nature than those of the shear loop.

This type, called a *prismatic loop,* is fundamentally different from the shear loop; the only feature the two types have in common is their circular shape. Other differences between shear and prismatic loops are summarized in Table 7.3.

**Table 7.3 Differences between Shear Loops and Prismatic loops**

| Characteristic | Shear loop | Prismatic loop |
|---|---|---|
| Location | On slip plane | Between close-packed planes |
| Peripheral dislocation type | Mixed | Edge |
| Central portion of loop | Perfect crystal lattice | Stacking fault |
| Mechanism of growth | Shear stress | Absorption of point defects |
| Orientation of Burgers vector | Parallel to loop | Perpendicular to loop |

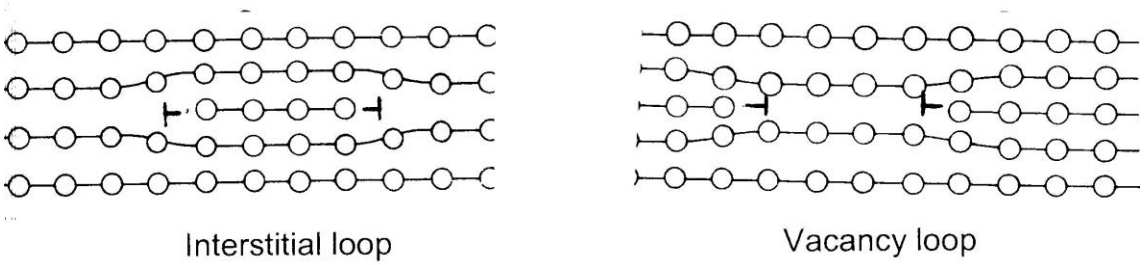


**Fig. 7.20 The two types of prismatic loops**

Corresponding to the two types of point defects, vacancies and interstitials, there are two types of prismatic loops. These are shown in Fig. 7.20. The interstitial loop consists of a disk-shaped layer (seen end-on in the figure) of atoms formed by assembling interstitial atoms from the bulk solid. The atom-layer agglomeration is thermodynamically more stable than the same number of atoms dispersed in the lattice as self-interstitials. Interstitial loops form only in solids bombarded by high-energy radiation (e.g., neutrons) because only this environment produces sufficient quantities of self-interstitials.

The right-hand sketch in Fig. 7.20 shows a prismatic loop formed by the collapse of a disk of vacancies on a close-packed plane. In common with the interstitial loop, the periphery of the vacancy loop is a circular edge dislocation with a Burgers vector perpendicular to the plane of the loop. However, the Burgers vectors of the two types are of opposite sign. Vacancy loops are also formed during irradiation. The interaction of irradiation-produced point defects with these two types of loops provides a mechanism for the phenomenon of irradiation growth in fuel elements containing uranium metal or zirconium alloys (see Chap. 19).

The existence of the loop requires a shear stress parallel to the Burgers vectors of the loop acting in the glide plane in Fig. 7.19. Such a shear stress produces radially outward forces on both the positive and negative pure edge portions. Because the shear stress acts parallel to the screw portions of the loop, the force due to the shear stress is radially outward over the entire periphery of the loop.

A force balance on a curved segment of the loop is identical to Eq (7.20) for the pinned dislocation. This result, however, is spurious. If the shear stress is removed, the loop collapses and disappears, thereby reducing the strain energy of the crystal. Yet Eq (7.20) indicates that as $\sigma_S \rightarrow 0$, $\Re$ becomes very large. At the opposite extreme, as the shear stress becomes large, the loop should expand because the force on its periphery is radially outward. Yet Eq (7.20) predicts that as $\sigma_S \rightarrow \infty$, the loop should shrink.

The conclusion from these contradictions is that the loop is not an equilibrium object. Rather, it is formed by an applied shear stress and, provided that the shear stress is maintained, will continue to expand until it encounters an obstacle or exits the body.

## 7.11 Dislocation Multiplication

### 7.11.1 Why a dislocation multiplication mechanism is needed

A shear stress acting on opposing faces of a solid (see Fig. 7.3) induces deformation only by moving only a fraction of the total dislocation density. In Fig. 7.21, all dislocations are of the edge type, so a shear stress $\sigma_S$ exerts a force only on dislocations lying in the z direction. Only edge dislocations oriented as shown in the figure (~ 1/3 of the total) experience an x-force. Eliminating screw dislocations (1/2) and pinned and immobilized dislocations (1/2), in all, only ~ 1/12 of the total dislocation density responds to an applied shear stress. It is possible to calculate the maximum shear strain if all of these dislocations leave the solid and cause macroscopic deformation.

The diagram on the upper left of Fig. 7.21 shows the unstrained solid with 4 slip planes each containing 4 properly-oriented mobile dislocation. The sequence shows the strain of the block as dislocations are removed from one slip plane at a time. The symbols for the edge dislocation indicate a half-plane of atoms extending perpendicularly from the slip plane to the upper or lower surface of the body.

- when the positive edge dislocations in the upper slip plane are all swept to the right, only the top layer of solid is displaced to the right (second diagram);
- when the negative dislocations in the second slip plane are acted on by the shear stress, the three lowest layers are displaced to the left but the second layer does not move ($3^{rd}$ diagram);
- movement of the positive dislocations in the third slip plane to the right carry with them all three uppermost layers, giving the deformed structure shown in the $4^{th}$ diagram.
- Finally, sweeping the remaining negative dislocations moves the bottom block to the left.

What remains of the dislocation-cleansed body is the shape deformed in shear shown in the last diagram. However, all of the dislocations have disappeared, so deformation of the body by the above mechanism is no longer possible.

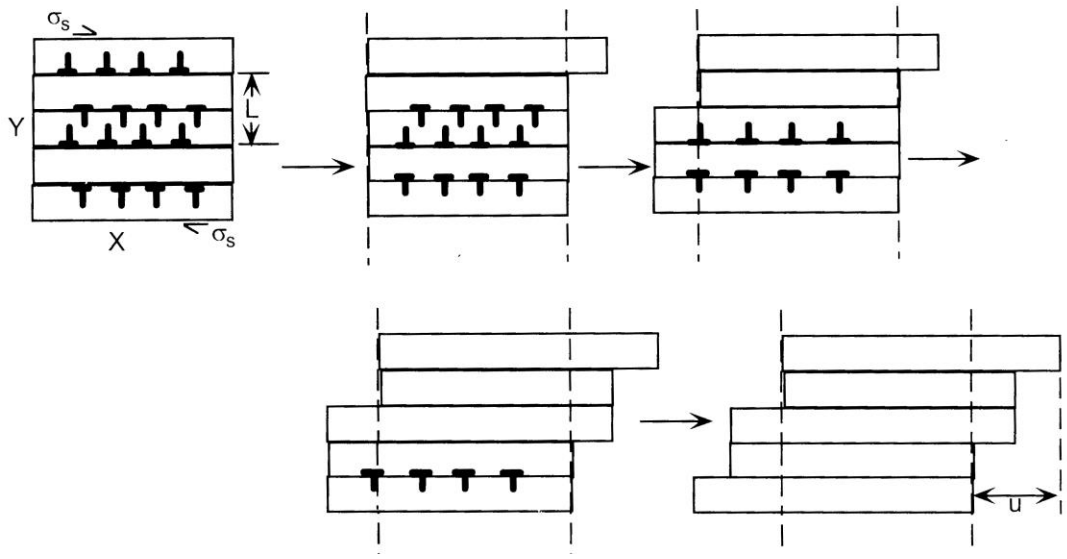


**Fig. 7.21 removal of mobile dislocations by a shear stress**

Example #4 Shear strain in a mechanical test

To generalize the above picture, consider the block of solid with the X and Y dimensions shown in the first diagram in Fig. 7.21 and unit length in the z direction. Assume n dislocations per unit length on each slip plane, each of which contain nX dislocations. When all dislocations are swept out of the crystal the x-displacement of each layer is nXb, where b is the Burgers vector. If L is the vertical distance between slip planes with dislocations of the same sign, Y/L planes have moved to the right. The x-shear displacement of the entire block (u in the last diagram of Fig. 7.21) is:

$$u = (nXb)(Y/L)$$

In a block of volume (X)(Y)(1), the total number of dislocations capable of movement is $N = XY\rho/12$, where $\rho$ is the total dislocation density and the factor of 12 accounts for the fraction that can glide when driven by the applied shear stress (see above).

Another measure of the total number of moveable dislocations is N = (nX)(2Y/L), the factor of 2 arising because the length L is the distance between every other slip plane (see Fig. 7.21). Equating these two measures of N gives:

$$\frac{n}{L} = \frac{\rho}{24}$$

Eliminating n/L from the above two equations and dividing by X to give the shear strain results in:

$$\varepsilon_x = \frac{u}{X} = \frac{1}{24}\rho bY$$

Using the following numerical values:

$\rho = 10^8$ cm$^{-2}$ (typical of annealed metals)

$b = 3\times10^{-8}$ cm (on the order of the interatomic spacing)

$Y = 1$ cm (characteristic dimension of mechanical test specimens)

The maximum shear strain obtained from the above equation is ~ 12%.

If deformation occurred solely by movement of pre-existing mobile dislocations, deformation should cease when all of these leave the body. In addition, the deformed body should have a lower dislocation density than the original specimen. Neither of these expectations is verified by experiment:

- shear strains well in excess of the 12% calculated in Example #4 are commonly observed (think of bending a paper clip);
- rather than *decreasing* the dislocation density by strain, a *higher* ρ is observed in deformed specimens.

The following section describes the mechanism for generating dislocations inside a solid undergoing plastic deformation.

### 7.11.2 The Frank-Read Source

Numerous mechanisms for generating dislocations are discussed in Ref. 6, Chap.8. Of these, the one proposed in 1950 independently and simultaneously by F. C. Frank and W. T. Read is the most important. The origin of this mechanism is the bowing of the pinned dislocation segment shown in Fig. 7.18 into a semicircle, or when the radius of curvature is one half of the separation of the pinning points. The stress at which this occurs is termed the *critical stress* or the *Frank-Read stress.* It is obtained from Eq (7.20) by setting $\Re = L/2$:

$$\sigma_{FR} = \frac{2Gb}{L} \tag{7.21}$$

Figure 7.22 shows the sequence of shapes of a pinned edge dislocation as the stress is increased up to and beyond the stability limit of Eq (7.21).

1. In the absence of a shear stress, a straight edge dislocation is fixed between the two pinning points (stage 1). This is the smallest length and therefore the lowest energy configuration.
2. For a shear stress less than the critical value, the dislocation assumes the shape of the arc in Fig. 7.18 and stage 2 in Fig. 7.22.
3. When the stress is exactly equal to $\sigma_{FR}$, the semicircular bowed dislocation is on the brink of instability (stage 3).

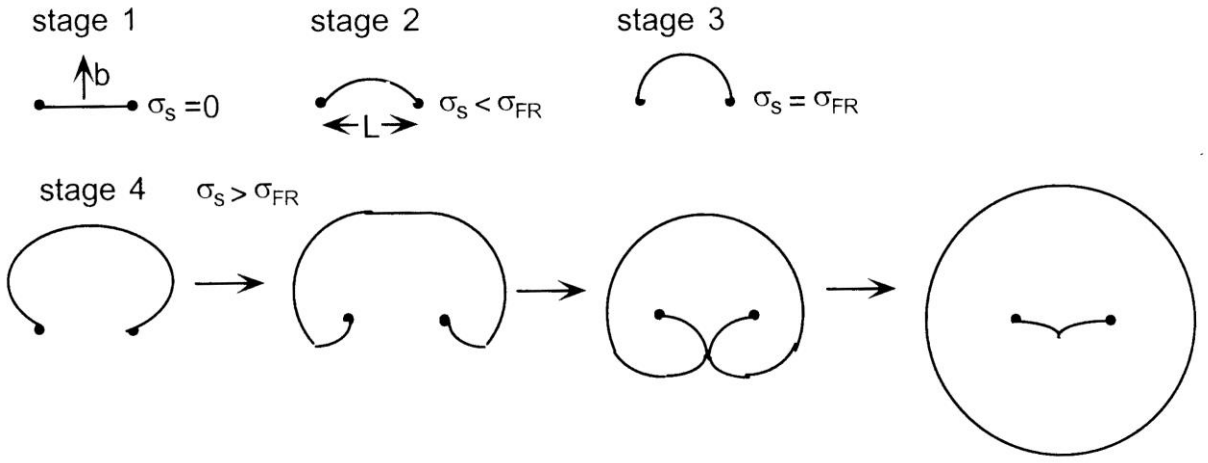

**Fig. 7.22 Operation of a Frank-Read Source**

4. If the stress is even slightly larger than $\sigma_{FR}$, the dislocation passes through a sequence of shapes, all of which are *unstable* for the same reasons outlined for the circular dislocation loop in Sect 7.10. As seen in stage 4 of Fig. 7.22, the loop swirls around the pinning points until the opposite lobes touch. The Burgers vector shown in stage 1 of Fig. 7.22 is the same for all parts of the loop, and at contact (stage 4), is parallel to the dislocation. Annihilation occurs because the contact at the third position of stage 4 is between two screw dislocations of opposite sign.

5. The products of the annihilation process are shown in the last drawing of stage 4 in Fig. 7.22. A circular loop freed from the pinning points becomes ever larger because the stress that initiated the process ( $> \sigma_{FR}$) exceeds that necessary to maintain and grow a loop. The other segment of dislocation resulting from the annihilation process is still attached to the pinning points and rapidly returns to the stage 1 shape.

As long as the stress is maintained $> \sigma_{FR}$, the 4-stage sequence of Fig. 7.22 is repeated. The result is continuous production of loops that expand at speeds determined by obstacles that hinder their motion.

## 7.12 Impediments to Dislocation Motion

Hindrance of dislocation movement is divided into two classes, *source hardening* and *friction hardening*[4]. *Source hardening* is caused by impurity atoms, precipitate particles, or other microstructural defects that are attached to the dislocation in its unstressed state. These entities "lock" dislocations such that initiation of motion or operation of Frank-Read sources requires a stress greater than that given by Eq (7.21). *Friction hardening* refers to the effect of obstacles of various types that impede the motion of mobile dislocations. The obstacles include other dislocations, foreign bodies ranging in size from impurity atoms to macroscopic precipitate particles and, in the case of metals irradiated by fast neutrons or fast ions, clusters of point defects. Friction hardening is further subdivided into *long-range* and *short-range* effects. Long-range friction hardening implies that the mobile dislocations do not directly contact the obstacle but feel its retarding force at a distance (Prob. 7.11). In short-range friction hardening, the mobile dislocations encounter obstacles lying in their slip planes.

### 7.12.1 Long-Range Friction Hardening

The conventional picture of this type of impediment to dislocation motion is the interaction of two parallel edge dislocations on different slip planes, as depicted in the right hand diagram of Fig. 7.16. A critical value of the applied shear stress is necessary to force mobile dislocation 2 past immobile dislocation 1. From Eqs (7.15) and (7.16), the retarding force exerted on 2 by 1 is:

[4] The term *hardening* refers to the increase in yield stress (the stress required to initiate dislocation movement) and to the continual increase in stress required to maintain dislocation motion as plastic strain increases

$$F_x = \frac{\Gamma b \sin(4\theta)}{4y} \tag{7.22}$$

where $\Gamma$ is the collection of elastic constants given by Eq (7.8). The maximum back force occurs at $\theta = \pi/8$, or:

$$(F_x)_{max} = \frac{\Gamma b}{4y} \tag{7.22a}$$

The forward force due to the applied shear stress is given by Eq (7.10), which in the present notation is:

$$(F_x)_{app} = \sigma_S b$$

When $(F_x)_{app}$ just exceeds $(F_x)_{max}$, dislocation 1 slips past dislocation 2 and goes on its way. With the help of Eq (7.8) the critical value of $\sigma_S$ is:

$$\left(\sigma_S^{crit}\right)_{friction} = \frac{\Gamma}{4y} = \frac{Gb}{8\pi(1-\nu)y} \tag{7.23}$$

The separation of the slip planes (y) is related to the dislocation density. From the discussion in Sect. 7.4, the separation of parallel dislocations in the unstressed solid should be of the order of the unit cell radius **R** given by Eq (7.4).

In a realistic collection of dislocations in a solid that is subject to an applied stress, two complications would need to be taken into account:

1. The force on a particular mobile dislocation in a random forest of dislocations is considerably more difficult to calculate than the above analysis for two parallel dislocations.
2. The angles identifying the direction of allowed motion of the mobile dislocation has to account for its slip system interacting with the force field of No. 1 above. That is, a critical resolved shear stress analogous to Eq (7.1) or Eq (7.1a) would need to be calculated.
3. Problem 7.11 is a simple example of two dislocations impeding a mobile one.

### 7.12.2 Dislocation Climb

Even if the applied shear stress is less than the critical value given by Eq (7.23), another mechanism is available for the mobile dislocation to pass an immobile one. By increasing the separation of the slip planes (y in Fig. 7.16) the critical shear stress is reduced until it eventually equals the applied shear stress. The process by which the mobile dislocation moves perpendicular to its slip plane is climb (see Sect. 7.3.4 and Fig. 7.11 in particular). With reference to the right-hand diagram of Fig. 7.16, the normal stress $\sigma_{xx}$ on dislocation 2 due to the presence of dislocation 1 is compressive (if $\sigma_{xx}$ is negative). The effect of this stress is to reduce the vacancy concentration at the core of dislocation 2 to a value below that in the bulk solid. This concentration difference generates a flux of vacancies to the dislocation, which responds by climbing upward, as shown in Fig. 7.11.

The key to establishing the reduction of the vacancy concentration at the dislocation core is the stress effect on the equilibrium vacancy concentration. This effect is analyzed in Sect. 4.2.1 and leads to Eq (4.9). In order to utilize this equation as a boundary condition on the vacancy diffusion equation, two modifications are needed. First, Fick's laws of diffusion must be cast in terms of the volumetric concentration of the diffusing species. Equation (4.9) is converted units of atoms/cm$^3$ by dividing both sides by the atomic volume $\Omega$. Second, the stress in Eq (4.9) is $\sigma_{xx}$ in Eq (7.6a). With these modifications and $v_V$ the specific volume of a mole of vacancies, the equilibrium vacancy concentration at the dislocation core is:

$$c_V(r_d) = c_V^{eq} \exp\left(\frac{\sigma_{xx} v_V}{R_g T}\right) \tag{7.24}$$

where $r_d$ is the radius of the dislocation core and $R_g$ is the gas constant.

$$c_V^{eq} = \exp\left(\frac{s_V}{R_g}\right)\exp\left(-\frac{E_V^f}{R_g T}\right)\frac{1}{\Omega} \tag{7.25}$$

is the equilibrium concentration in the stress-free solid.

The geometry in which a vacancy flux towards the dislocation ($J_V$) induced by the above concentrations is shown in Fig. 7.23. The radius of the unit cell **R** is given by Eq (7.4) in terms of the dislocation density.

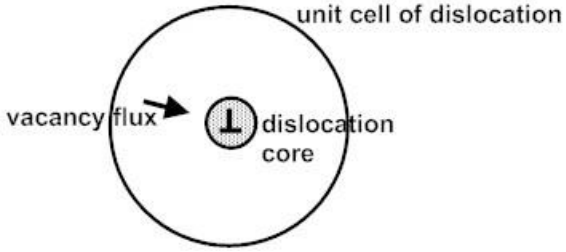


**Fig. 7.23 Vacancy diffusion in the unit cell of a dislocation**

The diffusion equation in the cylindrical annulus $r_d \le r \le \mathbf{R}$ is:

$$\frac{1}{r}\frac{d}{dr}\left(r\frac{dc_V}{dr}\right) = 0$$

The boundary conditions are given by Eq (7.24) at the dislocation core (radius $r_d$) and by Eq (7.25) at the periphery of the unit cell (radius R). The solution is:

$$\frac{c_V^{eq} - c_V}{c_V^{eq} - c_V(r_d)} = \frac{\ln(R/r)}{\ln(R/r_d)}$$

The flux of vacancies per unit length of dislocation is:

$$J_V = 2\pi r_d D_V \left( \frac{dc_V}{dr} \right)_{r_d} = \frac{2\pi}{\ln(R/r_d)} D_V \left( c_V^{eq} - c_V(r_d) \right)$$

The first term on the left hand side depends only on the geometry of the unit cell, and is written as:

$$Z_V = \frac{2\pi}{\ln(R/r_d)} \tag{7.26}$$

so that $J_V$ becomes

$$J_V = Z_V D_V \left( c_V^{eq} - c_V(r_d) \right) \tag{7.27}$$

For typical values R ~ $10^{-5}$ cm and $r_d$ ~ 3x$10^{-8}$ c, $Z_V$ ~ 1, a value that will be used throughout for numerical work.

$c_V(r_d)$ is expressed by Eq (7.24) in which the exponential term is represented by its one-term Taylor-series expansion. Eq (7.27) reduces to:

$$J_V = Z_V D_V c_V^{eq} \frac{|\sigma_{xx}| v_V}{R_g T} = \frac{Z_V D}{\Omega} \frac{|\sigma_{xx}| v_V}{R_g T} \tag{7.28}$$

where the self diffusion coefficient (D) has been substituted according to Eq (5.28) and site fraction and volumetric concentration are related by: $C_V^{eq} = c_V^{eq} \Omega$

The connection between the vacancy flux and the climb velocity can be deduced with the aid of Fig. 7.11. Let δt be the time required to remove one row of atoms from the bottom of the dislocation's half plane. The empty volume created (per unit length of dislocation) is $v_c \delta t\, b$, where $v_c$ is the climb velocity and b, the Burgers vector, is the approximate width of the half plane of atoms. The volume supplied by the vacancy flux during this time is $J_V \Omega \delta t$. From this volume balance, $v_c = J_V \Omega / b$. Substituting Eq (7.28) for $J_V$ gives the climb velocity:

$$v_c = \frac{Z_V D}{b} \frac{|\sigma_{xx} v_V|}{R_g T} \tag{7.29}$$

Example # 5: Two parallel edge dislocations on parallel slip planes initially 5 Burgers vectors apart are present in a specimen of iron. The applied shear stress pushing mobile dislocation 2 against immobile dislocation 1 in Fig. 7.16 is one half of the critical value given by Eq (7.23). Considering two temperatures, 500 K and 1000 K, how long will it take for dislocation 2 to climb until the critical stress is reduced to the actual stress?

In Eq (7.29), substituting dy/dt for $v_c$ and Eq(7.6a) for $\sigma_{xx}$ (in which r = y/sinθ) yields:

$$\frac{dy}{dt} = \frac{Z_V v_V D \Gamma}{b R_g T} \frac{\sin^2\theta(1+2\cos^2\theta)}{y} \tag{7.30}$$

$\Gamma$ is given by Eq (7.8).
In order to integrate the above equation, $\theta$ is expressed in terms of y by equating the back force on dislocation 2 due to dislocation 1 given by Eq (7.22) to the forward force $\sigma_S b$ exerted by the applied shear stress. $\sigma_S$ is equal to one-half of the initial critical shear stress given by Eq (7.23), or $\sigma_S = \Gamma/8y_o$, where $y_o$ is the initial separation of the slip planes. This yields:

$$\theta = \frac{1}{4}\sin^{-1}\left(\frac{1}{2}\frac{y}{y_o}\right) = \frac{1}{4}\sin^{-1}\left(\frac{1}{2}Y\right) \tag{7.31}$$

where $Y = y/y_o$. Equation (7.30) is made dimensionless using $y = y_o Y$ and $t = t^*\tau$, where the characteristic time for climb is given by:

$$t^* = \frac{b R_g T y_o^2}{Z_V v_V D \Gamma} \tag{7.32}$$

For dislocation 2 to overcome the back force of dislocation 1, it must climb to double the separation of the slip planes, or to Y = 2. This separation of the slip planes requires a dimensionless climb time given by:

$$\tau_f = \int_1^2 \frac{Y dY}{\sin^2\theta\,(1+2\cos^2\theta)}$$

Using Eq (7.31) to express $\theta$ in terms of Y, the integral is $\tau_f = 18.3$. The time for dislocation 2 to escape dislocation 1 is $t_f = 18.3t^*$. In order to evaluate $t^*$ from Eq (7.32), the following properties of iron are used:

G = 73 GPa (room temperature value)
b = 0.3 nm
$\nu = 0.33$
These values yield $\Gamma = 5.2$ N/m (using Eq (7.8)).
$Z_V = 1$
$y_o = 5b = 1.5$ nm
$v_V = 6.6\text{x}10^{-6}$ $m^3$/mole
$R_g = 8.314$ J/mole-K
$D = 1.9\text{x}10^{-4}\exp(-28{,}800/T)$ $m^2/s$

At 1000 K, Eq (7.32) gives a characteristic climb time of $t^* = 2.7$ ms, or the time for the dislocation to climb to the point that the blocking dislocation is circumvented is 50 ms. At this temperature, climb is so rapid that friction hardening is negligible. At 500 K, on the other hand, the decrease in the self-diffusion coefficient is so pronounced that the comparable escape time is 2 ½ millennia. The only way that a blocked mobile dislocation can pass by an immobile one is to increase the applied shear stress until it exceeds the critical value.

### 7.12.3 Jogs

So far, only the interaction forces between parallel dislocations have been considered[5]. However, even the simplified representation of dislocations in Fig. 7.13 shows that moving dislocations are sure to encounter dislocations at an angle other than $0^o$. When this occurs, the two dislocations stop at some distance apart or physically touch each other. If the stress is sufficiently high, one dislocation can cut through the other and both can continue on their way, albeit with more difficulty than before intersection.
There are a large number of combinations of interacting dislocations.

i) Each combination requires a different stress for the crossed dislocations to disengage;
ii) Each combination leaves one or both disfigured by a *jog*, or kink, in the initially straight or continuously curved line;
iii) upon disengagement from each other, one or both require a larger stress to continue moving than prior to the intersection;
iv) the angle of approach of the two dislocations can be anywhere between 0 and $90^o$.

In order to provide a rudimentary understanding of dislocation intersection, six combinations grouped into two sets are shown in Fig. 7.24. The interacting dislocations are at right angles to each other. In the two sets of interactions shown in Fig. 7.24, the three vertical dislocations, which are the same in both sets, are assumed to be immobile. In the set on the left, a horizontal edge dislocation has cut through the three vertical ones. In the right hand set, the moving dislocation is a pure screw.

Moving edge dislocation (left-hand diagram in Fig. 7.24)
**1(edge).** The intersection of moving edge dislocation $b_e$ with vertical edge dislocation $b_1$ produces a jog in the latter, but not in the former. The length of the jog in $b_1$ is of the order of an atomic spacing[6]. It is treated as a small segment of a dislocation that maintains the Burgers vector of $b_1$. Since the jogged section is perpendicular to $b_1$, it must be of edge character (see Fig. 7.2a). Moreover, because the Burgers vector $b_1$ lies in the slip plane of the segment, the jog does not interfere with the glide motion of the vertical edge dislocation that contains it.

[5] Sect. 7.9 without applied stress; Sect 7.10 with applied stress for screw dislocations; earlier in this section with applied stress for edge dislocations
[6] It may appear odd that a jog one atomic diameter in length has the properties of a line defect. In fact it does not (Ref. 6, p. 131). However, enough of the properties of a true line defect are at least partially retained by the nanometer-length line that treating it as a dislocation segment is useful.

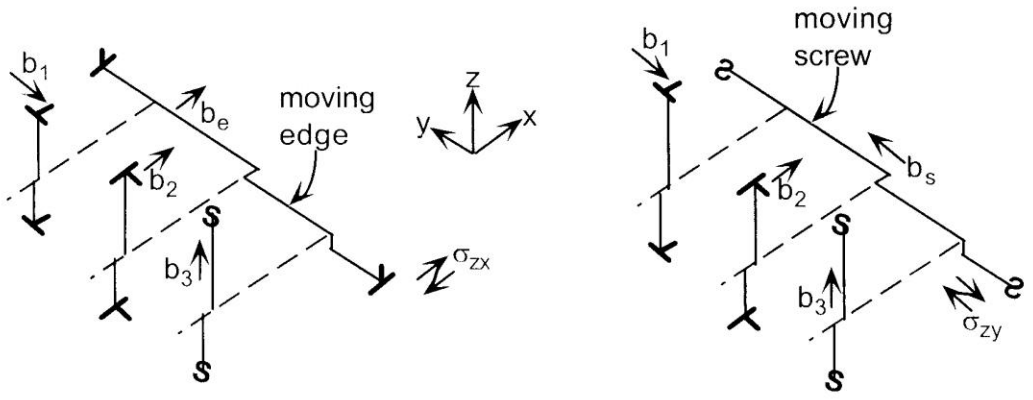


**Fig. 7.24 Intersection of three vertical dislocations by a moving edge dislocation (left) and by a moving screw dislocation (right)**

**2(edge)** In the next case, the Burgers vectors $b_2$ and $b_e$ are parallel. The jogs that appear on both dislocations are parallel to the Burgers vectors, and consequently are short segments of screw dislocations. The shear stress responsible for moving $b_2$ and $b_e$ are parallel to the jogged segments, which move along the main dislocations in a manner similar to the motion of the wave in a garden hose when one end is given a sharp shake. Neither jog impedes the motion of the main dislocation.

**3(screw)** When the moving edge dislocation $b_e$ cuts through the vertical screw dislocation $b_3$, the jogged sections are perpendicular to the Burgers vectors of the original dislocations. Hence, the segments are of edge character. An edge dislocation can slip only in a plane containing both the line and its Burgers vector, which is true for the jogs in both $b_3$ and $b_e$. However, for slip, the jog must move in a direction perpendicular to itself. This is true of the jog in $b_e$, which therefore does not hinder motion of the moving edge dislocation. The extra half-plane (or more precisely, half-row) edge jog in $b_3$ lies in the plane perpendicular to the main screw dislocation. Depending on the orientation of the vertical shear stress component (i.e., $\sigma_{zx}$ or $\sigma_{zy}$), the main screw dislocation is capable of glide in a direction either perpendicular to $b_e$ or parallel to it. In the former case, the edge-like jog would need to move parallel to itself, which it normally cannot do. In the latter case, movement of the jog in $b_3$ is by climb (because the short "half-plane" of the edge jog is perpendicular to $b_3$). Such movement necessitates a higher stress than that for glide, and in addition, requires absorption or emission of point defects.

The consequences of the dislocation intersections in the three cases analyzed above illustrate the following general rules:

1. Jogs in pure edge dislocations do not impede glide motion of the main dislocation. However, the slip plane of the jogged section may not be as energetically favored as that of the main dislocation.

2. Jogs in pure screw dislocations hinder movement of the parent dislocation, which requires a higher applied stress to drag along the recalcitrant jog.

Moving screw dislocation (right-hand diagram in Fig. 7.24)

The shear stress $\sigma_{zy}$ is required to move the $b_S$ screw dislocation decorated with a number of edge jogs in the x direction. The applied shear stress acts in the y direction in the plane perpendicular to the z axis. The edge jogs glide freely up and down the main screw dislocation. Some jogs are positive and others are negative. Jogs of opposite sign annihilate each other until only one kind remains. Since edge dislocations of the same sign repel one another, the jogs assume equidistant positions along the screw dislocation.

At low shear stress the mobile segments of the screw dislocation between the jogs are pinned by the jogs, and can only bow out in the manner shown in Fig. 7.18. If the applied shear stress is sufficiently large, the array of jogs moves by climb along with the main screw dislocation. At temperatures low enough that the point defects are immobile, this process leaves a trail of point defects in the wake of each climbing jog. Figure 7.25 shows a screw dislocation moving in the x direction emitting vacancies The climbing jogs leave behind extra atom planes (gray rectangles in Fig. 7.25).

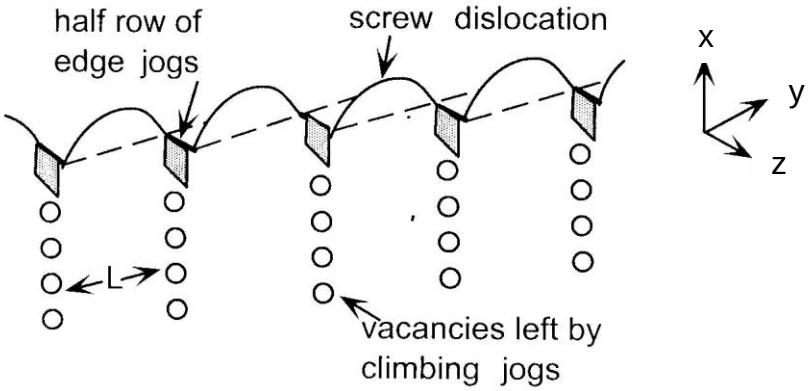


**Fig. 7.25 Mechanism of movement of a jogged screw dislocation**

The stress required to initiate the climb process shown in Fig. 7.25 is obtained by equating the energy to create a vacancy to the work done by the interjog segment of the screw dislocation as it moves one Burgers vector in its glide direction.

The energy required to create a vacancy beneath a jog is assumed to be the same as that for a normal lattice vacancy (Sect. 4.2) even though the surroundings of the vacancy are quite different in the two cases. A normal vacancy resides in an otherwise unperturbed lattice site, whereas the jog vacancy sits in the highly disrupted core of an edge dislocation. In addition, the energy of vacancy formation is replaced by:

$$E^f_{V,jog} = 0.2Gb^3$$

The right hand side of this equation is the energy added to that of the dislocation by the presence of the jog; $Gb^2$ is the energy per unit length of a dislocation (Eq 7.9), and if the jog is regarded as a dislocation of length b, its energy is $Gb^3$. The factor of 0.2 in the above equation arises from the much reduced range of the stress field due to the jog compared to that around an ordinary dislocation. However, there is no physical reason why the energy of the jog can be taken to be the energy to form a vacancy. The above evaluation of the formation energy of a jog vacancy is given without physical justification in Ref. 8, p. 105 and Ref. 9, p. 597.
Nonetheless, the approximation is remarkably accurate; for copper, G = 46 Gpa and b = 0.26 nm, for which the above equation gives $E^f_{V,jog}$ = 90 kJ/mole. The normal vacancy formation energy for copper is $E^f_V$ = 100 kJ/mole

Creation of a vacancy beneath the jog is accompanied by glide of the screw dislocation a distance b, the Burgers vector. On a per-jog basis, the work required is the force per unit length of dislocation given by Eq (7.12), in which the shear stress is $\left(\sigma_S^{crit}\right)_{jog}$. Multiplying by L, the interjog spacing (Fig. 7.25), the work performed by the stress is:

$$W = Lb^2\left(\sigma_S^{crit}\right)_{jog}$$

Equating the work to the energy expended in producing the vacancy, the critical stress to move the screw dislocation by forcing the jogs to climb is:

$$\left(\sigma_S^{crit}\right)_{jog} \cong 0.2\frac{Gb}{L} \qquad (7.33)$$

### 7.12.4 Obstacles

Metals used in nuclear reactors contain impediments to dislocation motion that are introduced into the solid by a variety of means, including:

i) expressly during fabrication - intermetallic precipitates in Zircaloy are in this class;
ii) incomplete purification during fabrication - commercial aluminum is stronger than high-purity aluminum;
iii) during operation – the voids, bubbles and defect clusters produced in most metals by irradiation by high-energy neutrons or ions are the most notable examples of this class of obstacles.

Irrespective of how they are introduced into the metal, obstacles have several features in common. First, they can be approximated by spheres or points for the purpose of analysis. Second, they impede or stop the motion of dislocations. Third, as a consequence of the second, their effect is to harden the metal and at the same time render it more brittle.

Obstacles range in size from individual impurity atoms, small clusters of point defects 1 – 2 nm in size found in metals irradiated by fast neutrons at low temperature and large precipitate particles. These obstacles have in common a stress field around them that either attracts or repels the dislocation. In the latter case, the applied stress must be large enough to

overcome the repulsive force; in the former case, the applied stress must be able to tear the dislocation away from its attractive trap.

Two mechanisms are available to dislocations to overcome an obstacle.
1) if the obstacle is small enough, the dislocation can cut through it;
2) the dislocation can bow around an array of large obstacles.
The cutting mechanism is not treated here; brief discussions of this process can be found in Sect. 18.5 of Ref. 3 and in Sect. 10.6(a) of Ref. 5.

The stress required to push a dislocation through an array of impenetrable spherical obstacles depends on their center-to-center spacing in the slip plane, L. This in turn is a function of the obstacle's radius R and its number density in the solid, N. These two quantities can be related to their separation distance L with the aid of the sketch on the left of Fig. 7.26.

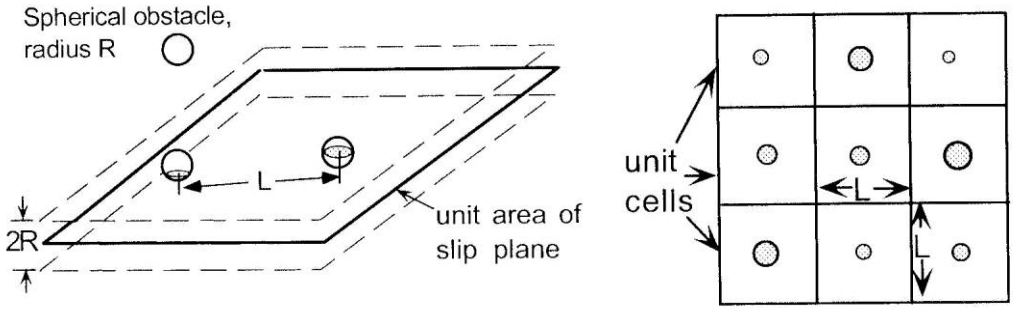


**Fig. 7.26 The intersections of volume-distributed spherical objects with a plane**

A sphere whose center lies within the square volume 2Rx1x1 will touch the plane. The number of spheres within this volume is 2RN, which is also the number of objects intersecting the unit plane.

The right-hand sketch of Fig. 7.26 changes the random positions of the circular intersections of the obstacles and the slip plane to the centers of unit cells. The unit cell is a square of side L with an object's intersection in its center. The area of this unit cell, $L^2$, divided into the unit area of the plane is also the number of intersections of the objects with unit slip plane. Equating these two expressions and solving for L yields:

$$L = (2RN)^{-1/2} \tag{7.34}$$

The average radius of the intersections shown as shaded circles in Fig. 7.26 is $\pi R/4$.

Figure 7.27 shows how a straight dislocation pushed to the right by the applied shear stress interacts with the array of obstacle intersections on its slip plane. Not only the intersections of the volume-distributed obstacles placed on a square grid, but their radii are all accorded the average value of $\pi R/4$. The dislocation interacts with the obstacles at their peripheries, whose separation distance $l$ is less than the center-to-center distance of Eq (7.34) by the average diameter:

$$l = L - \pi R/2 = (2RN)^{-1/2} - \pi R/2 \tag{7.35}$$

The sequence of events by which the dislocation passes through the obstacle array on its slip plane can be broken into 4 stages. The straight dislocation approaches the obstacle array (no. 1 in Fig. 7.27) and bows out between them (no. 2). If the applied stress is too small to bow the line into a semicircle, the dislocation line

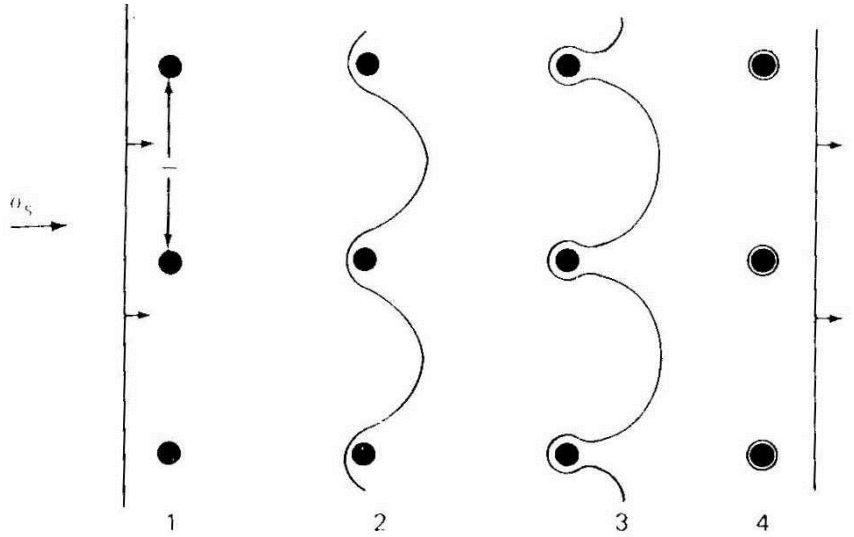


**Fig. 7.27 A dislocation moving through an array of obstacles in its glide plane**

is stuck in this configuration with the sections bowed to a radius of curvature given by Eq (7.22). At an applied stress sufficiently large to bow the dislocation between obstacles into a semicircle (no. 3), the shape becomes unstable and expands in the same manner as the Frank-Read source shown in Fig. 7.22. When the portions of adjacent expanding bows touch, the dislocation line is reformed and proceeds on its way, leaving behind a circular dislocation loop of the type shown in Fig. 7.5 around each obstacle (no. 4). The stress required to reach the instability of stage 3 is given by Eq (7.22) with $\Re = l/2$:

$$\left(\sigma_S^{crit}\right)_{obstacle} = 2Gb / l \tag{7.36}$$

where $l$ is given by Eq (7.35).

As successive dislocation lines pass through the obstacle array, the residual loops accumulate around the obstacles and effectively increase their size. Because of this growth in the size of the obstacles, their separation decreases below the initial value $l$, and the according to Eq (7.36), the stress to pass the barrier increases. This effect contributes to the macroscopic phenomenon of work-hardening.

### 7.12.5 Locking and Unlocking

The addition of impurity atoms, whether they be substitutional or interstitial, hardens metals by hindering the start of edge dislocation motion (they have no effect on screw dislocations). The impurities tend to accumulate around edge dislocations because at this location the system's energy is reduced. The solid above the slip plane (i.e., in the section containing the extra half-

plane of atoms) is in compression while the solid below the slip plane is in tension. A substitutional impurity atom that is larger than the host atoms generates a compressive stress field in the immediate vicinity. Consequently, it has a tendency to accumulate on the tensile side of the slip plane, because the compressive stress is relieved by the dislocation's tensile stress and vice versa. For the same reason, substitutional impurity atoms smaller than the host atoms tend to migrate to the compressive side of the slip plane. Interstitial impurity atoms are small compared to the host atoms (e.g., carbon, nitrogen, boron) yet they always create a compressive stress field around them because they are not in a regular lattice site. Consequently, interstitial impurities tend to collect just below the end of the edge dislocation's half plane (i. e., in the open space in the middle diagram of Fig. 7.2).

In order for edge dislocations to accumulate impurity atoms, high temperature and/or long times are needed. This can occur during fabrication as the molten metal cools and solidifies, the principal example being carbon in steel. Alternatively, high temperatures during operation of the component or very long times at low temperatures (called aging) can produce the same result.

Analysis of this phenomenon is based on interstitial impurities, although similar results apply to substitutional alloying atoms. The first step is to determine the interaction energy between the interstitial atom and the edge dislocation. The interstitial atom is regarded as an oversized rigid sphere inserted into a hole in the solid of radius $R_o$, roughly equal to the cube root of the volume of an interstitial site in the host crystal structure. Insertion of an interstitial atom into this hole increases the radius of the hole to $(1+ \varepsilon)R_o$, $\varepsilon$ being << 1 to an extent depending on the radius of the interstitial atom and the size of the interstitial sites in the host lattice. The volume change of the solid in the immediate vicinity of the interstitial is:

$$\Delta V = \frac{4}{3}\pi[(1+\varepsilon)^3 R_o^3 - R_o^3] \cong 4\pi R_o^3 \varepsilon$$

Expansion of the medium in the vicinity of an edge dislocation performs work against the hydrostatic component of the dislocation's stress field. From Eqs (7.6) this is:

$$\sigma_h = \frac{1}{3}(\sigma_{rr} + \sigma_{\theta\theta} + \sigma_{zz}) = \frac{Gb}{3\pi}\left(\frac{1+\nu}{1-\nu}\right)\frac{\sin\theta}{r}$$

The work done in expanding against this stress is the interaction energy, $E_i = \sigma_h \Delta V$. Multiplying the above two equations and assuming $\nu = 1/3$ gives[7]:

$$E_I = \frac{8}{3} Gb\varepsilon R_o^3 \frac{\sin\theta}{r} \qquad (7.37)$$

The interstitial atoms are attracted to the atom half plane at the underside of the slip plane because $\sin\theta < 0$ at this location and so $E_I$ is negative (the geometry defining $\theta$ and r is that shown on the right in Fig. 7.16, with the interstitial replacing dislocation #2).

[7] The exact value of the numerical coefficient in Eq (7.37) is 4 (Ref. 6, p. 172 et seq).

Because of the reduction of energy with decreasing r, interstitials will tend to congregate around the underside of the edge dislocation. Not all interstitials in the vicinity of the dislocation can occupy the minimum energy sites, which according to Eq (7.37), is at $\sin\theta = -1$ and r is at its minimum value. The latter, designated $r_o$, is the distance separating the interstitial located just below the half plane of the dislocation and the terminating atoms of the half plane (i.e., $r_o$ is the open space in the middle sketch of Fig. 7.2). First, the minimum energy location is not an unsaturable sink; there is only one interstitial site for every terminating atom of the dislocation half plane. Second, if $E_I$ is of the order of thermal energy ($\sim R_gT$), vibrations of the host atoms in the lattice (phonons) establish an equilibrium distribution of interstitials around the dislocation:

$$C_I(r) = C_I(\text{bulk})\exp(-E_I/R_gT) \qquad (7.38)$$

$C_I(r)$ is the fraction of interstitial sites at distance r from the dislocation that are occupied by an interstitial atom. $C_I$(bulk) is the interstitial site fraction far from the dislocation line. Interstitials congregate beneath the dislocation's half plane since here $E_I < 0$.

Equation (7.38) fails when $C_I(r)$ equals or exceeds unity at any r. In this case, the interstitial sites just below the half plane are fully occupied. The tensile stress field normally associated with the solid below the slip plane of an edge dislocation now becomes greatly reduced because of the interstitials in the locations just below the half plane. The interaction energy with this interstitial-saturated edge dislocation and interstitials in the lattice is greatly reduced. What remains is a dislocation "locked" by the row of underlying interstitials attached to it. The applied shear stress required to break the dislocation is called the *unlocking stress*. Calculation of this stress is given in Ref. 5, p. 216, and will be summarized here.

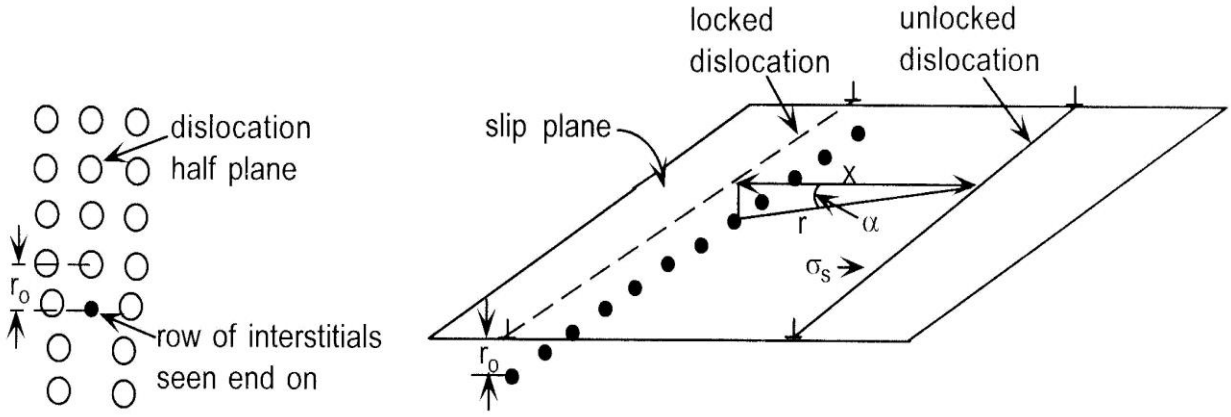


**Fig 7.28 Row of interstitials filling all sites below the half plane of an edge dislocation. End-on view (left); the unlocking process (right)**

Figure 7.28 shows an edge dislocation pushed by applied shear stress $\sigma_S$ to a distance x along its slip plane from the row of interstitial atoms to which it was initially locked. The interaction energy between the unlocked dislocation line and a single interstitial atom given by Eq (7.37) can be written in compact form as:

$$E_I = A\frac{\sin\theta}{r} \tag{7.37a}$$

where A is the collection of constants in Eq (7.37). The angle $\alpha$ in the triangle in Fig. 7.28 is equal to $-\theta$, so that $\sin\theta = -\sin\alpha = -r_o/r$ and Eq (7.37a) becomes:

$$E_I = -A\frac{r_o}{r^2} = -\frac{Ar_o}{x^2 + r_o^2} \tag{7.37b}$$

The force between the dislocation line and the single interstitial atom intersected by the triangle in Fig. 7.28 is the derivative of Eq (7.37b). Since interstitial atoms in the row are separated by approximately one Burgers vector, there are 1/b interstitials per unit length of the row. The force between the dislocation located a distance x from its locked position and the interstitials in a unit length of the row is:

$$F(x) = -\frac{1}{b}\frac{dE_I}{dx} = -\frac{2Ar_o}{b}\frac{x}{\left(x^2 + r_o^2\right)^2}$$

The force is negative, meaning that the row of interstitial atoms restrains the movement of the dislocation. Counter-intuitively, the force is not a maximum when x = 0. The above function of x has a maximum at $x = r_o/\sqrt{3}$ ; since $r_o$ is of the order of a Burgers vector, the maximum force occurs at a very small x displacement from the dislocation's locked position. The maximum restraining force on the unlocked dislocation (in N/m) is:

$$F_{max} = -\frac{3\sqrt{3}A}{8br_o^2}$$

$F_{max}$ is the maximum force between the entire dislocation line and a unit length of the row of interstitials. By symmetry, it also represents the maximum retarding force on a unit length of the unlocked dislocation exerted by the entire row of interstitial atoms.

For the dislocation to become unlocked, the opposing applied force (given by Eq (7.18)) must equal $F_{max}$, or the unlocking shear stress is:

$$\left(\sigma_S^{crit}\right)_{unlock} = \frac{3\sqrt{3}A}{8b^2r_o^2} = \sqrt{3}\,\varepsilon\frac{R_o^3}{br_o^2}G \tag{7.38}$$

### 7.12.6 Summary

The four mechanisms that impede the motion of dislocations analyzed in this section are summarized in Table 7.4, which also gives best-estimate numerical values for the critical stresses (relative to the shear modulus) .

**Table 7.4 Numerical comparison of the mechanisms hindering dislocation motion In formulas, b = Burgers vector = 0.3 nm; R = radius of dislocation unit cell = $\rho^{-1/2}$**

| **Mechanism** | $\sigma_s^{crit}/G$ **(formula)** | **Equation** | $\sigma_s^{crit}/G$ **(value)** | **Parameter values** |
|---|---|---|---|---|
| Friction | $\frac{b/R}{8\pi(1-\nu)}$ | 7.23 | $2\times10^{-5}$ | $\rho = 10^8$ cm$^{-2}$ |
| Jogs | $0.2\frac{b}{L}$ | 7.33 | $6\times10^{-4}$ | L = 2R = separation of jogs on screw dislocation – Fig.7.25; $\rho = 10^{10}$ cm$^{-2}$ |
| Obstacles | $2b/l$ | 7.36 | $6\times10^{-4}$ | $l$ = 1 μm = spacing of obstacles on slip plane |
| Locking | $\sqrt{3}\,\varepsilon\frac{R_o^3}{br_o^2}$ | 7.38 | $4\times10^{-3}$ | ε = 0.02 = fractional radial expansion of interstitial site when occupied; $r_o$ = b = separation of interstitial row and bottom of half plane of the edge dislocation – Fig. 7.26; $R_o^3 = \Omega/4 = 1.2\times10^{-23}$ cm$^3$ $R_o$ = interstitial site radius |

The critical stresses due to friction and jogs depend only on the presence of other dislocations at a reasonably high density. These critical stresses are in satisfactory accord with the critical resolved shear stress measured on single crystals (Sect. 7.3). The critical stresses from the obstacle and locking mechanisms are very sensitive to the concentration of impurities in the crystal.

The first three mechanisms are active for moving dislocations. It is possible that a mobile dislocation is subject to all three at once. In this case, the critical shear stress to maintain motion would be the sum of the critical stresses for the individual mechanisms.

The critical stress for unlocking a dislocation acts only to initiate motion of a dislocation. Once freed from the row of impurity atoms, the stress to keep the dislocation moving may be lower than the unlocking stress. This is observed in engineering stress-strain tests and is called the *yield drop.*

## Appendix - Stress notation in Cartesian and Cylindrical Coordinates

The following chart summarizes the meaning of the subscripts on the stresses.
In $\sigma_{ij}$, i denotes the plane on which the stress acts and j is the direction in which it acts.

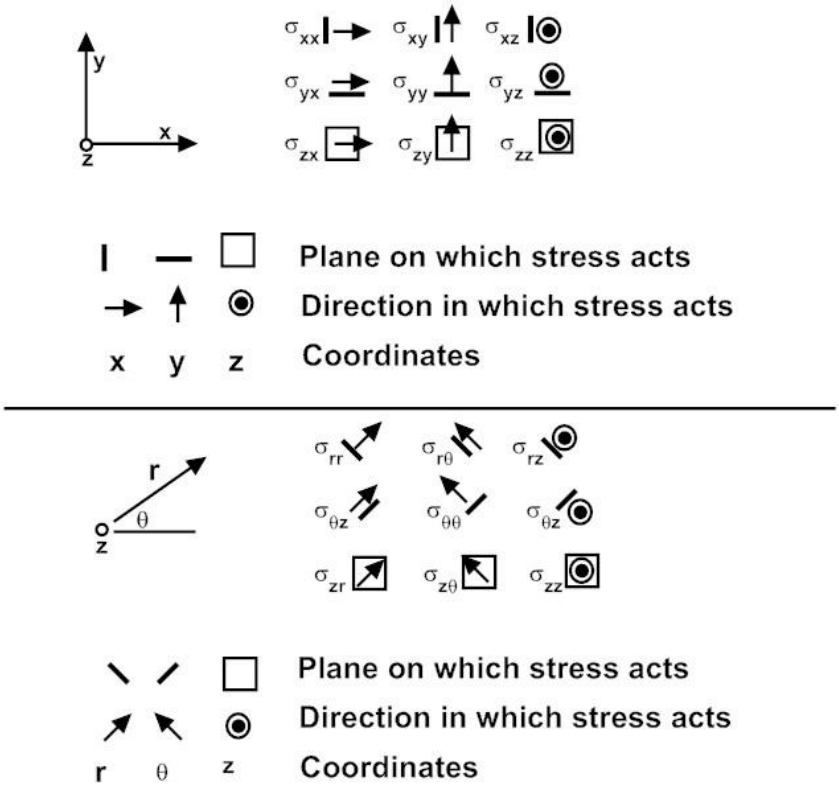

## References


1. L. H. Van Vlack, M*aterials Science for Engineers,* Addison Wesley (1970)

2. C. R. Barrett, W. D. Nix and A. S. Tetelman, *The Principles of Engineering Materials*, Prentice-Hall (1973)

3. D. R. Olander, *Fundamental Aspects of Nuclear Reactor Fuel Elements*, U. S. Technical Information Center, TID-26711-P1 (1976)

4. M. M. Eisenstadt, *Introduction to Mechanical Properties of Materials*, Macmillan Co. (1971)

5. D. Hull, *Introduction to Dislocations*, Pergamon Press (1965)

6. Johannes and Julia R. Weertman, *Elementary Dislocation Theory*, Macmillan Co. (1964)

7. W. D. Callister, Jr., *Materials Science and Engineering*, Wiley & Sons (1985)

8. Jacques Friedel, *Dislocations*, Pergamon Press (1964)

9. J. P. Hirth, *Theory of Dislocations*, Wiley (1982)

10. J.A. Shackelford, Introduction to Materials Science, $4^{th}$ ed., (1995)

# Problems

## 7.1

The arrow in the drawing shows the Burgers vector of the edge dislocation.

(a) What is the crystal structure ?
(b) What plane is shown in the drawing? (see Fig. 3.5)
(c) What is the notation for the Burgers vector shown (Sect. 7.3.2)?
(d) What is the magnitude of the Burgers vector?
(e) Show that (d) is consistent with (c).

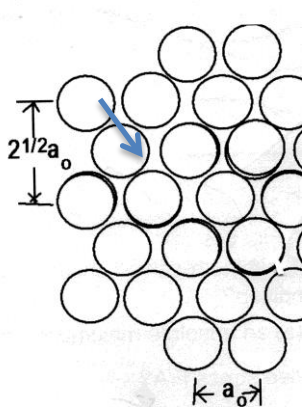


## 7.2

What is the force per unit length between parallel edge dislocations with perpendicular Burgers vectors? The Burgers vectors in Fig. 7.16 are parallel. For this problem, rotate the tee of one of the dislocations by $90^o$.

## 7.3

The periphery of the interstitial loop in Fig. 7.6 is called a Frank partial dislocation. For the fcc crystal structure, what is the designation of this dislocation?

## 7.4

(a) For a specified $\phi$ in Fig. 7.7a, at what $\varphi$ is the resolved shear stress a maximum?
(b) At what value of $\phi$ is the result of part (a) a maximum?

## 7.5

(a) The critical resolved shear stress of single-crystal copper is 0.5MPa. A specimen of this metal is loaded in tension in the [110] direction. At what applied tensile stress will (111)[101] slip occur?

(b) A single-crystal bar of a bcc metal is cut into a tensile test specimen with the (100) planes perpendicular to the applied force. The slip system is (110)[111] and the critical resolved shear stress is known. At what $\sigma_{app}$ does slip occur?

**7.6**

The edge dislocations in Fig. 7.16 are five Burgers vectors apart (i.e., y = 5b). The lower dislocation is immobile and the other (mobile) one is subject to an applied shear stress $\sigma_S$ = 0.1G. What is the separation r at equilibrium (in units of b)?

**7.7**

(a) What is the magnitude of the Burgers vector in bcc Fe and hcp Zr?
(b) What are the self-energies per unit line length of these dislocations?
Shear moduli: $G_{Fe}$ = 64 GPA; $G_{Zr}$ = 39 GPa

**7.8**

In the face-centered tetragonal lattice (Fig. 3.7), slip occurs in the (001) (bottom) plane.

(a) What is the most likely slip direction?
(b) What is the designation of the edge Burgers vector?
(c) What is the magnitude of this Burgers vector? The smallest lattice parameter is 0.28 nm

**7.9**

The drawing shows a shear loop (Fig. 7.5) in the center of a cube with sides consisting of dislocation lines. The resolved shear stress acting in the plane of the loop expands the loop until it contacts the vertical dislocation sides of the cube. l

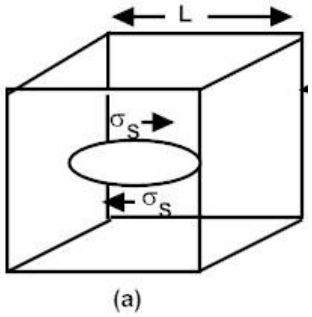


(a) Draw the subsequent positions of the loop if the resolved shear stress is greater than the critical value.
(b) What stress is required to expand the loop by bowing around the trees?

**7.10**

(a) What are the forces (per unit length), both climb and glide, that each dislocation exerts on the other.

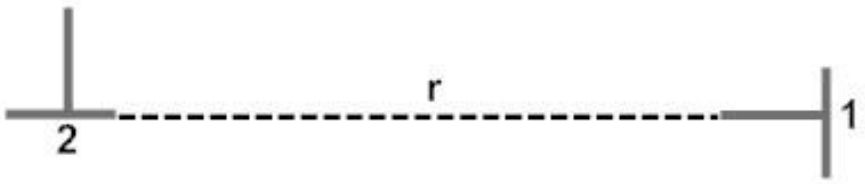


(b) Show that the forces balance.

(c) What are the climb and glide forces (per unit length) on dislocation 2 due to the presence of dislocation 1?

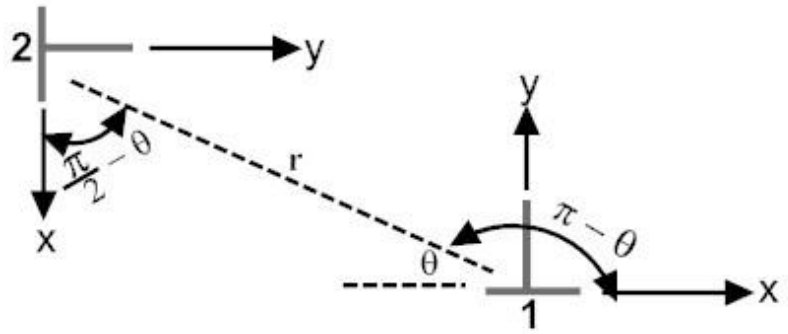


k;

(d) Show that the forces calculated in parts (a) and (c) are consistent.

## 7.11

The mobile edge dislocation in the drawing is pushed to the right along a slip plane between immobile dislocations 1 and 2 by a shear stress $\sigma_S$. What is the equilibrium distance x?